INL/EXT-19-53559
Revision 0

AGR-2 Irradiation Experiment Fission Product Mass Balance

John D. Stempien
Paul A. Demkowicz

April 2019

The INL is a
U.S. Department of Energy
National Laboratory
operated by
Battelle Energy Alliance

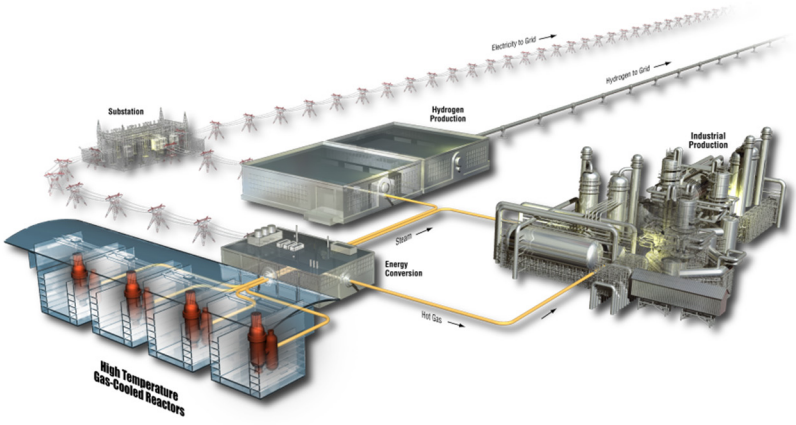

Idaho National Laboratory

INL/EXT-19-53559
Revision 0

AGR-2 Irradiation Experiment Fission Product Mass Balance

John D. Stempien
Paul A. Demkowicz

April 2019

Idaho National Laboratory
INL ART Program
Idaho Falls, Idaho 83415

http://www.inl.gov

Prepared for the
U.S. Department of Energy
Office of Nuclear Energy
Under DOE Idaho Operations Office
Contract DE-AC07-05ID14517

INL ART Program

AGR-2 Irradiation Experiment Fission Product Mass Balance

INL/EXT-19-53559
Revision 0

April 2019

Author:

John D. Stempien
AGR TRISO Fuel PIE Technical Lead

4/17/2019
Date

Technical Reviewer: (Confirmation of mathematical accuracy, and correctness of data and appropriateness of assumptions.)

Paul A. Demkowicz
AGR Program Technical Director

4/17/19
Date

Approved by:

Travis R. Mitchell
ART Project Manager

4/17/19
Date

Michelle T. Sharp
INL Quality Engineer

4/17/19
Date

REVISION LOG

Rev.	Date	Affected Pages	Revision Description
0	04/17/2019	All	New document.

SUMMARY

The Advanced Gas Reactor (AGR) program is in the process of qualifying tristructural isotropic (TRISO)-coated uranium carbide/uranium oxide (UCO) fuel for use in high-temperature gas-cooled reactors (HTGRs) in the United States. The second AGR irradiation (AGR-2) started in the Advanced Test Reactor (ATR) in June 2010 and was completed in October 2013. The first AGR irradiation (AGR-1) tested fuel produced on laboratory scale equipment, but the AGR-2 TRISO-coated fuel particles were produced on an industrial scale and then overcoated and compacted into cylindrical compacts using laboratory-scale processes. Both UCO and UO_2 fuels were irradiated in AGR-2 so that their performance could be compared. The UCO fuel was in Capsules 2, 5, and 6, and the UO_2 fuel was in Capsule 3. (Capsules 1 and 4 were French and South African fuel, respectively. These fuels will not be discussed.) UCO burnups ranged from 7.3 to 13.2 % fissions per initial metal atom (FIMA), and compact time-averaged, volume-averaged (TAVA) irradiation temperatures ranged from about 1000°C to 1300°C. UO_2 compact burnups ranged from 9.0 to 10.7 % FIMA, and compact TAVA temperatures ranged from about 1000 to 1060°C.

Components from each US AGR-2 irradiation capsule were analyzed to determine the inventory of fission products retained in or released from the fuel compacts. The irradiation capsule shells, through tubes, graphite compact holders, and graphite spacers were analyzed for gamma-emitting fission products, primarily isotopes of Ag, Cs, and Eu. Except for the spacers, these components were also analyzed for beta-emitting Sr-90. To give measured-to-calculated fractions (M/C), measured values were compared to the values predicted from physics calculations to have been produced in the fuel.

Ag-110m was significantly released through intact TRISO coatings in all capsules. It was measured on every component in each of the US AGR capsules (Capsules 2, 3, 5, and 6). Summing the measured silver from all components *except* the fuel gives Ag-110m releases from the compacts that ranged from 13% for Capsule 3 to 70% for Capsule 5. Re-normalizing the Ag-110m measured outside of the compacts by the M/Cs from summing Ag-110m measured on all components *plus* the compacts accounts for potential biases in the physics predictions of Ag-110m production and/or the possible incomplete recovery of Ag-110m from the irradiation capsule metallic components. This gives an adjusted range of Ag-110m release: 11% for Capsule 3, up to 75% for Capsule 7. Re-normalized Capsule 5 Ag-110m releases decreased from 70% to 60%. Plotting the re-normalized M/Cs versus compact TAVA irradiation temperature shows an increase in Ag-110m release at 1100°C. This is consistent with observations from AGR-1 and AGR-3/4. From these data, however, it could not be determined if the inherent Ag-110m retention of UO_2 or UCO was different.

Measured Cs-134 releases ranged from a capsule fraction of about 4.0E-5 to 8.7E-5 (1.5 to 3.3 particle equivalents) in the UCO fuel. A fraction of 1.96E-6 (0.036 particle equivalents) was measured outside of the UO_2 fuel compacts. Plotting the Cs-134 measured outside of the fuel compacts versus the average compact TAVA irradiation temperature in each capsule gave a linear dependence. This suggests that the majority of the cesium measured outside of the fuel compacts could be from a few exposed kernels (either from in-pile SiC failures or from as-fabricated SiC layer defects).

Eu-154 and Sr-90 were generally measured in similar quantities outside of the fuel compacts. The Eu-154 fraction outside of the fuel in Capsule 6 was determined from a minimum detectable activity (MDA) to be < 2.9E-4. The measured Sr-90 outside of the fuel in Capsule 6 was 8.2E-5. For Capsule 5 the measured Eu-154 release fraction was 2.7E-5 (the bounding fraction including MDA contributions was < 4.9E-5), and the measured Sr-90 release fraction was 6.4E-5. For UO_2 Capsule 3, the Eu-154 release fraction was < 3.8E-4 based on an MDA, and the Sr-90 release fraction was measured to be 1.3E-4. In Capsule 2, the hottest capsule in AGR-2, the measured Eu-154 release fraction was 3.7E-2, and the Sr-90 release fraction was 1.2E-2. This is evidence of significant release of these two isotopes from intact TRISO coatings in Capsule 2. The measured Sr-90 releases from UCO compacts in Capsules 5 and 6 were less than from the UO_2 compacts in Capsule 3. Little Eu-154 was measured outside of the compacts

(especially in Capsules 3, 5, and 6 which had similar irradiation temperatures); thus it is difficult to compare UCO and UO_2 Eu-154 retention from the available data. Over the same temperature range, the UCO fuel compacts have similar or better Sr-90 retention than the UO_2 compacts.

These data can be used to help interpret data obtained during irradiation (such as fission gas release-to-birth ratios) and in other post-irradiation examinations (PIE) (e.g., as-irradiated analyses and safety testing). Of interest is the quantity of fission products that was released from the fuel particles but retained within the compact matrix. As-irradiated compact destructive analyses can determine the inventory retained in the matrix, and combining this with the measured inventories outside of the fuel compacts from the mass balances in this report can give an estimate of the total fission product inventory released from the fuel particles

ACKNOWLEDGEMENTS

The authors gratefully acknowledge the work of Hot Fuel Examination Facility staff that disassembled the AGR-2 test train to retrieve the samples. Dr. Jason Harp performed the gamma scans of the compact holders and compacts. Staff at the Analytical Laboratory performed gamma scanning of the capsule spacers, analyses of the capsule shells and through tubes, and burn leach of the holders. Measured values were compared to physics predictions performed by Dr. Jim Sterbentz.

CONTENTS

SUMMARY vii

ACKNOWLEDGEMENTS ix

ACRONYMS xv

1. INTRODUCTION 1
   1.1 Program Purpose 1
   1.2 Current Status of AGR Program Irradiations 1
   1.3 AGR-2 Fuel Description 2
   1.4 AGR-2 Test Train and Irradiation 4

2. PIE METHODS 6
   2.1 Non-destructive Analysis Methods 6
      2.1.1 Metrology of Holders and Compacts 6
      2.1.2 Precision Gamma Scanning 6
      2.1.3 Spacers Gamma Counting 6
   2.2 Destructive Analysis Methods 7
      2.2.1 Metallic Hardware: Through Tubes and Capsule Shells 7
      2.2.2 Graphite Holders 7
      2.2.3 Spacers 10

3. CAPSULE MASS BALANCE RESULTS 11
   3.1 Calculations with Data and Representation of Results 11
   3.2 Capsule 2 13
   3.3 Capsule 3 15
   3.4 Capsule 5 17
   3.5 Capsule 6 19
   3.6 Summary of Inventories Released from Fuel 20

4. DISCUSSION 22
   4.1 Comparison of Compact Holder PGS Results with Burn-leach 22
   4.2 Silver Mass Balance 23
   4.3 Cesium Mass Balance 27
   4.4 Europium and Strontium Mass Balances 28

5. CONCLUSIONS AND FUTURE WORK 31

6. REFERENCES 33

Appendix A Analytical Laboratory Report Numbers 35

FIGURES

Figure 1. TAVA irradiation temperatures versus burnup for compacts from the AGR-1 and AGR-2 irradiations. AGR-1 burnups and temperatures from (Sterbentz 2013) and (Hawkes 2014a), respectively. AGR-2 burnups and temperatures from (Sterbentz 2014) and (Hawkes 2014b), respectively. 2

Figure 2. X-radiographs of U.S. UCO (compact LEU09-OP2-Z002, left) and UO_2 (compact LEU11-OP2-Z018, right) compacts taken from the same compact lots used in the AGR-2 irradiation. Note the visibly lower packing fraction of the UO_2 compact. Images taken from Hunn et al. 2010. 3

Figure 3. Radial cross section diagram of a U.S. AGR-2 irradiation capsule. 4

Figure 4. Gamma spectrometry system in Hot Cell 4 at the AL. 7

Figure 5. Crushed graphite holders from Capsules 3, 6, and 5 prior to the start of oxidation. 9

Figure 6. Capsules 3, 6, and 5 graphite holders after oxidation. Tall-form beakers were put inside overburden containers after chemical reactions with the quartz tall-form beakers started. 9

Figure 7. Some of Capsule 2 graphite holder pieces and plastic container in aluminum weighing tray. 10

Figure 8. Fractional inventory of Ag-110m measured outside of the fuel compacts. 24

Figure 9. Total inventory of Ag-110m measured across all irradiation capsule components and the fuel compacts compared to Ag-110m production predicted from physics calculations. 24

Figure 10. Three representations of the fraction of Ag-110m measured outside of the fuel compacts as a function of the compact-averaged TAVA irradiation temperature. 26

Figure 11. Measured-to-calculated Ag-110m fraction in each compact in each capsule versus compact TAVA irradiation temperature. 26

Figure 12. Fractional inventory of Cs-134 measured outside of the fuel compacts. Patterned fill indicates values derived from MDAs. 27

Figure 13. Capsule fractions of Eu-154 measured on components outside of the fuel compacts. Left: highlights Capsule 2. Right: highlights Capsules 3, 5, and 6. Patterned fill indicates values derived from MDAs. 29

Figure 14. Capsule fractions of Sr-90 measured on components outside of the fuel compacts. Left: highlights Capsule 2. Right: highlights Capsules 3, 5, and 6. 29

Figure 15. Fractions of Eu-154 and Sr-90 measured outside of the fuel compacts as a function of the compact-averaged TAVA irradiation temperature. Open symbols for Eu-154 indicate values derived from MDAs. 30

TABLES

Table 1. Summary of selected AGR-2 UCO and UO_2 TRISO particle properties and compact properties. 3

Table 2. Burnups, fluences, and irradiation temperatures for compacts from AGR-2 Capsules 2, 3, 5, and 6. Thermal values from (Hawkes 2014b). Burnup and fluence values from (Sterbentz 2014). 5

Table 3. Comparison of received/recovered graphite holder weights at AL to calculated pre-irradiation weights. 10

Table 4. Capsule 2 mass balance for selected isotopes. 13

Table 5. Measurement error for each component and propagated measurement error for the sums of detected values. 14

Table 6. Capsule 3 mass balance for selected isotopes. 15

Table 7. Measurement error for each component and propagated measurement error for the sums of detected values. 16

Table 8. Capsule 5 mass balance for selected isotopes. 17

Table 9. Measurement error for each component and propagated measurement error for the sums of detected values. 18

Table 10. Capsule 6 mass balance for selected isotopes. 19

Table 11. Measurement error for each component and propagated measurement error for the sums of detected values. 20

Table 12. Summary of the total fraction of selected isotopes released from the fuel compacts in each capsule. 20

Table 13. Relative error of the total measured fractions given in Table 12. 21

Table 14. Ratio of fraction of selected fission products measured from burn-leach of graphite compact holders to the fraction measured from PGS. 22

Table 15. Summary of the number of particles' worth of Cs-134 outside of the fuel compacts in each capsule. These values were excerpted from Table 4, Table 6, Table 8, and Table 10. 28

ACRONYMS

AGR	Advanced Gas Reactor
AL	Analytical Laboratory
ART	Advanced Reactor Technologies
ATR	Advanced Test Reactor
EOI	end of irradiation
FIMA	fissions per initial heavy metal atom
HFEF	Hot Fuel Examination Facility
HTGR	high temperature gas-cooled reactor
ICP-MS	inductively-coupled plasma mass spectrometry
INL	Idaho National Laboratory
IPyC	inner pyrolytic carbon
M/C	measured-to-calculated ratio
MDA	minimum detectable activity
OPyC	outer pyrolytic carbon
ORNL	Oak Ridge National Laboratory
PGS	Precision Gamma Scanner
PIE	post-irradiation examination
SiC	silicon carbide
TAVA	time-averaged volume-averaged
TRISO	tristructural isotropic
UCO	uranium oxycarbide
UO_2	uranium dioxide

AGR-2 Irradiation Experiment Fission Product Mass Balance

1. INTRODUCTION

1.1 Program Purpose

The Advanced Gas Reactor (AGR) Fuel Development and Qualification Program was established to perform research and development on tristructural isotropic (TRISO)-coated particle fuel to support deployment of a high-temperature gas-cooled reactor (HTGR). This work continues as part of the Advanced Reactor Technologies (ART) TRISO Fuel Program. The overarching goal of the ART AGR program is to provide a baseline fuel qualification data set to support licensing and operation of an HTGR. To achieve these goals, the program includes the elements of fuel fabrication, irradiation, post-irradiation examination (PIE) and safety/heating testing, fuel performance modeling, and fission product transport (INL 2017). Several fuel irradiation experiments have been performed at the Advanced Test Reactor (ATR) at Idaho National Laboratory (INL), and a fourth irradiation began in February 2018. These experiments are intended to provide data on fuel performance under irradiation, support fuel fabrication process development, qualify fuel for operating and accident conditions, provide irradiated fuel for accident testing, and support development of fuel performance and fission product transport models.

1.2 Current Status of AGR Program Irradiations

The first two AGR fuel irradiation experiments (AGR-1 and AGR-2) had similar test train designs, and one objective was to test the performance of uranium oxycarbide (UCO) TRISO-coated particle fuel over a range of irradiation temperatures and burnups. The UCO fuel kernels are a heterogeneous mixture of uranium carbide and uranium oxide. Figure 1 shows the time-averaged, volume-averaged (TAVA) irradiation temperature and burnup for each AGR-1 and AGR-2 fuel compact. Burnup is given as percent fissions per initial metal atom (FIMA). AGR-2 TRISO coatings were fabricated using conditions derived from the AGR-1 Variant 3 fuel. The AGR-1 coatings were produced at the laboratory-scale, but AGR-2 coatings were produced in a large (150-mm diameter), industrial-scale coater (Demkowicz 2013, INL 2017).

In addition to AGR UCO fuel (in Capsules 2, 5, and 6), the AGR-2 experiment also had UO_2 fuel (in Capsule 3) to compare the performance of UCO versus UO_2 fuel and to compare to UO_2 fuel performance observed historically in the German TRISO fuel program.[a] AGR-1 was irradiated in the B-10 position in ATR from December 2006 to November 2009 (Collin 2015a). AGR-2 was irradiated in the B-12 position of ATR from June 2010 to October 2013 (Collin 2018a). The major elements of AGR-1 PIE are complete (Demkowicz et al. 2015). AGR-2 PIE began in July 2014, is still in-progress, and encompasses as-irradiated analyses, reirradiations, heating testing, microscopy, and other activities.

The third irradiation experiment, AGR-3/4, was designed to investigate the migration of fission products in fuel compact graphitic matrix and reactor graphite components. AGR-3/4 was irradiated in the northeast flux trap of ATR, from December 2011 to April 2014 (Collin 2015b). The experiment consisted of fuel compacts containing TRISO-coated driver-fuel particles similar to AGR-1 baseline fuel (Collin 2015b; Hunn and Lowden 2007; Hunn et al. 2014) and designed-to-fail (DTF) particles that are designed to release fission products during irradiation, which then migrate through the surrounding cylindrical rings of graphitic matrix and nuclear-grade graphite. AGR-3/4 PIE is in progress and will provide data to support refinement of fission product transport models and HTGR source-term analyses

[a] The AGR-2 irradiation had 6 irradiation capsules. Capsules 2, 3, 5, and 6 were US AGR capsules. Capsules 1 and 4 were French and South African fuel, respectively (Collin 2018a). Capsule 1 and 4 fuel compacts are not shown in Figure 1.

(Demkowicz 2017). The fourth irradiation experiment, AGR-5/6/7 (Collin 2018b), started in ATR in February 2018 and serves as the fuel qualification irradiation.

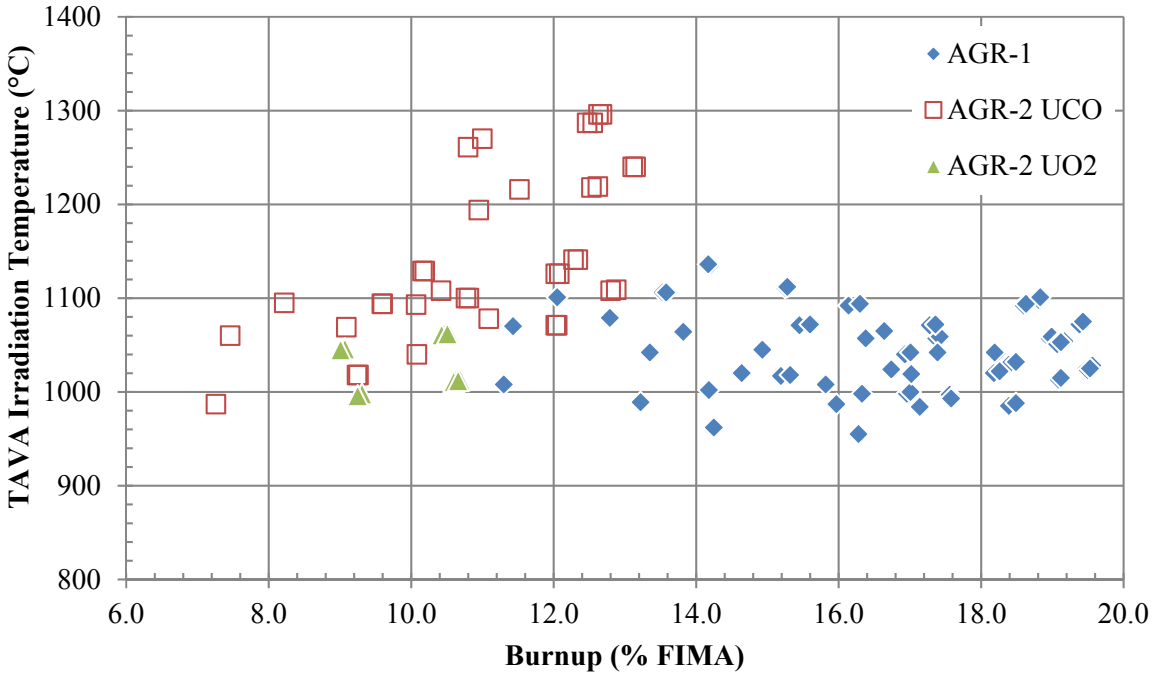

Figure 1. TAVA irradiation temperatures versus burnup for compacts from the AGR-1 and AGR-2 irradiations. AGR-1 burnups and temperatures from (Sterbentz 2013) and (Hawkes 2014a), respectively. AGR-2 burnups and temperatures from (Sterbentz 2014) and (Hawkes 2014b), respectively.

1.3 AGR-2 Fuel Description

AGR-2 Capsules 2, 5, and 6 contained only U.S. UCO fuel, and Capsule 3 contained only U.S. UO_2 fuel. Both the kernels and the TRISO coatings were fabricated at BWXT in Lynchburg, Virginia. The UCO kernels were approximately 425 µm in diameter and were enriched to 14.0 weight % U-235. The UO_2 kernels were fabricated to dimensions and enrichments comparable to the German and South African pebble-bed HTGR fuel designs. UO_2 kernels were approximately 500 µm in diameter and were enriched to 9.60 weight % U-235. Once the TRISO coatings had been applied to the kernels, the particles were overcoated and compacted into cylinders nominally 25.1 mm long and 12.3 mm in diameter at Oak Ridge National Laboratory. UCO compacts had a volume packing fraction of 37%, and UO_2 compacts had a volume packing fraction of 23%. Figure 2 shows x-ray radiographs of a UCO compact with a 37% packing fraction (left) and a UO_2 compact with a 23% packing fraction (right). There were approximately 3176 TRISO-coated fuel particles in each UCO compact and 1543 fuel particles in each UO_2 compact. A summary of major TRISO particle and fuel compact properties is given in the *AGR-2 Irradiation Test Final As-Run Report* (Collin 2018a). Detailed characterization data of the as-fabricated kernels, particles, and compacts have been compiled in reports referenced in (Collin 2018a). Select fuel properties from tables in Appendix A of (Collin 2018a) are given below in Table 1.

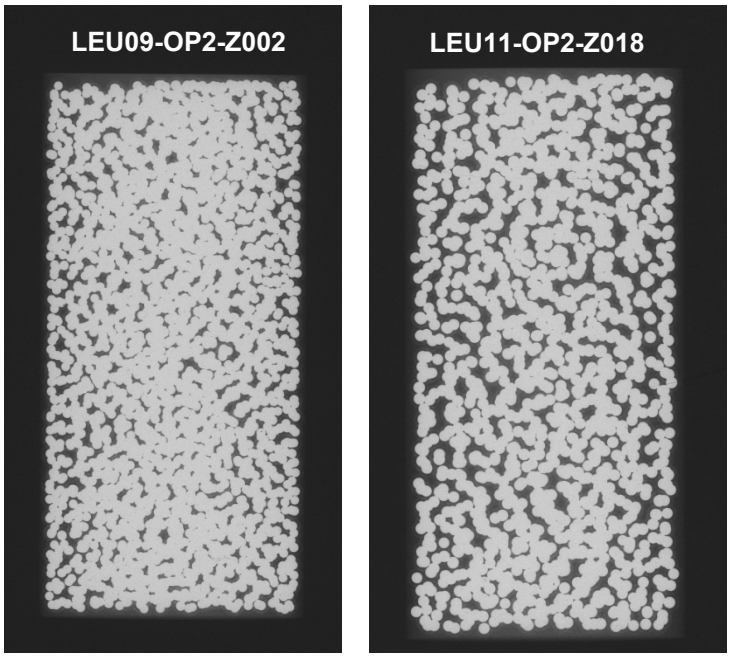

Figure 2. X-radiographs of U.S. UCO (compact LEU09-OP2-Z002, left) and UO_2 (compact LEU11-OP2-Z018, right) compacts taken from the same compact lots used in the AGR-2 irradiation. Note the visibly lower packing fraction of the UO_2 compact. Images taken from Hunn et al. 2010.

Table 1. Summary of selected AGR-2 UCO and UO_2 TRISO particle properties and compact properties.

Property	Mean Value and Standard Deviation	
	UCO	UO_2
U-235 enrichment (wt %)	14.029 ±0.026	9.600 ±0.010
Kernel diameter (μm)	426.7 ±8.8	507.7 ±11.9
Buffer thickness (μm)	98.9 ±8.4	97.7 ±9.9
IPyC thickness (μm)	40.4 ±2.5	41.9 ±3.2
SiC thickness (μm)	35.2 ±1.2	37.5 ±1.2
OPyC thickness (μm)	43.4 ±2.9	45.6 ±2.4
Overall particle diameter (μm)	873.2 ±23	953.0 ±28
Number of particles per compact	3176	1543
Particle volume packing fraction	37	23
IPyC: inner pyrolytic carbon OPyC: outer pyrolytic carbon		

1.4 AGR-2 Test Train and Irradiation

The AGR-2 irradiation test train consisted of six capsules, numbered 1 through 6, from the bottom to the top of the ATR core. Each capsule was approximately 150 mm (6 inches) long and 36 mm (1.4 inches) in diameter. Capsules 2, 3, 5, and 6 were U.S. AGR capsules. Figure 3 shows a cross section of a U.S. AGR-2 irradiation capsule. Each capsule was independently controlled for temperature and independently monitored during irradiation for fission product gases. AGR-2 compact holders utilized borated graphite to act as a burnable poison to reduce capsule powers during the early phases of the irradiation and to reduce power peaking throughout the irradiation. Niobium through tubes were used to pass thermocouples and instrumentation along the test train. Each capsule shell ("SST Pressure Boundary") was made of stainless steel. At the top and bottom of each capsule were graphite spacers (not shown in Figure 3) that sandwiched the compact holder and compacts.

The US graphite compact holders had three holes or "stacks" of compacts. Stacks 1 and 2 faced toward the center of the ATR core, while Stack 3 faced away from the center of the ATR core. Each stack had four compacts stacked on top of one another so that, in total, each capsule contained 12 fuel compacts. Compacts within a given stack were numbered from bottom to top (1 being the bottom and 4 being the top). Compacts were given three-digit identifiers, where the first digit is the capsule number, the second digit is the level of the compact within its stack, and the third digit is the stack number. For example, Compact 3-2-1 was in Capsule 3, at Level 2, in Stack 1. Table 2 summarizes the calculated fast fluence, burnup, and different time-averaged irradiation temperatures for each compact in Capsules 2, 3, 5, and 6.

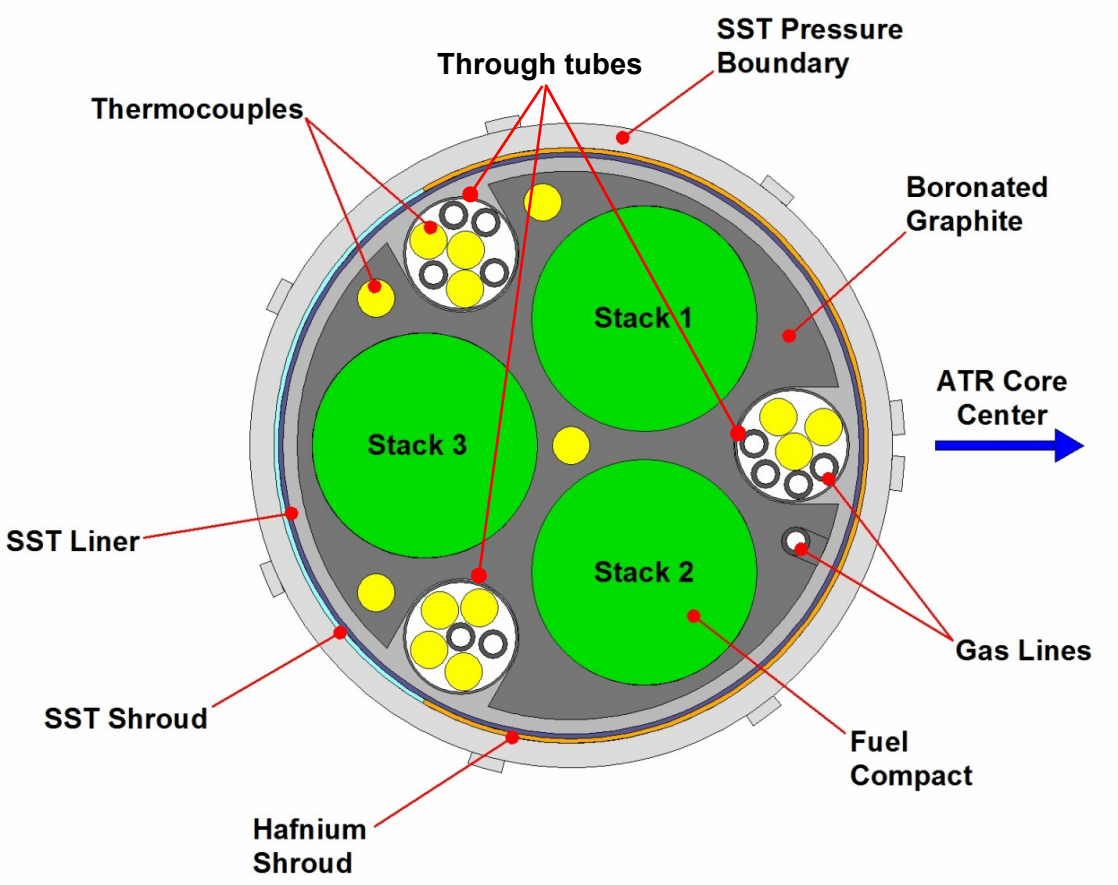

Figure 3. Radial cross section diagram of a U.S. AGR-2 irradiation capsule.

Table 2. Burnups, fluences, and irradiation temperatures for compacts from AGR-2 Capsules 2, 3, 5, and 6. Thermal values from (Hawkes 2014b). Burnup and fluence values from (Sterbentz 2014).

Capsule	Stack	Compact	Burnup (% FIMA)	Neutron Fluence (10^{25} n/m^2, E > 0.18 MeV)	TA[a] Minimum Temp. (°C)	TAVA[a] Temp. (°C)	TA[a] Peak Temp. (°C)
6	1	4	9.24	2.20	891	1018	1106
		3	9.59	2.42	1003	1094	1160
		2	10.16	2.60	1044	1129	1183
		1	10.77	2.73	964	1100	1178
	2	4	9.26	2.21	894	1018	1106
		3	9.60	2.43	1006	1094	1160
		2	10.19	2.61	1047	1129	1183
		1	10.81	2.73	968	1100	1178
	3	4	7.26	1.94	868	987	1080
		3	7.46	2.14	970	1060	1134
		2	8.22	2.30	1012	1095	1157
		1	9.09	2.42	941	1069	1152
6 Average			9.30	2.39	868	1074	1183
5	1	4	12.05	3.12	923	1071	1168
		3	12.03	3.28	1016	1126	1197
		2	12.28	3.38	1032	1141	1209
		1	12.8	3.41	956	1108	1202
	2	4	12.03	3.14	927	1071	1168
		3	12.08	3.29	1021	1126	1197
		2	12.34	3.39	1037	1141	1210
		1	12.88	3.42	962	1109	1203
	3	4	10.08	2.77	901	1040	1143
		3	10.07	2.91	986	1093	1172
		2	10.42	3.00	1003	1108	1184
		1	11.09	3.03	936	1078	1177
5 Average			11.68	3.18	923	1101	1210
3	1	4	10.62	3.47	901	1013	1085
		3	10.46	3.49	997	1062	1104
		2	10.43	3.47	995	1061	1104
		1	10.6	3.41	900	1011	1083
	2	4	10.69	3.5	904	1013	1085
		3	10.54	3.53	999	1062	1105
		2	10.51	3.51	998	1062	1104
		1	10.66	3.45	903	1012	1084
	3	4	9.31	3.10	891	998	1073
		3	9.07	3.11	981	1046	1092
		2	9.01	3.09	980	1045	1092
		1	9.25	3.05	889	996	1072
3 Average			10.10	3.35	889	1032	1105
2	1	4	13.11	3.44	1069	1240	1343
		3	12.63	3.42	1195	1296	1360
		2	12.47	3.35	1185	1287	1353
		1	12.53	3.21	1050	1218	1324
	2	4	13.15	3.47	1074	1240	1343
		3	12.68	3.46	1199	1296	1360
		2	12.55	3.39	1189	1287	1354

Capsule	Stack	Compact	Burnup (% FIMA)	Neutron Fluence (10^{25} n/m^2, E > 0.18 MeV)	TA[a] Minimum Temp. (°C)	TAVA[a] Temp. (°C)	TA[a] Peak Temp. (°C)
		1	12.62	3.25	1055	1219	1324
	3	4	11.52	3.08	1054	1216	1324
		3	11.00	3.06	1171	1270	1342
		2	10.80	2.99	1161	1261	1335
		1	10.95	2.88	1034	1194	1305
2 Average			12.17	3.25	1034	1252	1360
TA: time-averaged							

2. PIE METHODS

AGR-2 PIE mass-balance activities were aimed at measuring the fission product inventories of each component of the irradiation test train so that the release of fission products from the fuel compacts could be quantified. Of the components shown in Figure 3, the stainless steel capsule shells ("SST Pressure Boundary"), through tubes, and graphite compact holders ("Boronated graphite") were analyzed for fission products. Additionally, the graphite spacers immediately above and below the compact holder were also analyzed. These analyses took place either at the Analytical Laboratory (AL) at the Materials and Fuels Complex or at the Hot Fuels Examination Facility (HFEF) also at the Materials and Fuels Complex. Appendix A lists the AL report numbers associated with these analyses.

2.1 Non-destructive Analysis Methods

2.1.1 Metrology of Holders and Compacts

At the completion of the irradiation in ATR, the test train was sent to HFEF. The test train was gamma scanned prior to disassembly to verify that fuel and components within the test train had not shifted. All irradiation capsules were disassembled, the compacts and holders were separated, and dimensional measurements were taken of the holders and compacts (Ploger et al. 2015).

2.1.2 Precision Gamma Scanning

Compacts and compact holders were gamma scanned on the Precision Gamma Scanner (PGS) located at HFEF at INL to determine their inventories of gamma-emitting fission products (Harp et al. 2016a, Harp et al. 2016b). The measured compact and compact holder inventories of gamma-emitting fission products were compared to the inventories predicted from physics calculations in (Sterbentz 2014). Burnup evaluations were also made for each compact and compared to the physics predictions (Harp et al. 2016a, Harp et al. 2016b).

Additional compact holder scans were performed. In a technique called gamma emission computed tomography, the compact holders were rotated and gamma scans were acquired at multiple azimuths, at a specific axial location that had elevated levels of cesium activity. These scans were then mathematically reconstructed to produce two-dimensional maps of fission product intensities in the holders (Harp et al. 2016a, Harp et al. 2016b). Knowing the axial location and the compact stack that the elevated cesium activity was near, specific compacts were targeted for destructive PIE.

2.1.3 Spacers Gamma Counting

The top and bottom of each compact holder both had two spacers: one graphite spacer (either H-451 or NGB-25) and one Grafoil spacer (Graftech Grade GTA). Upon disassembly of each capsule, the two top spacers were packaged together, and the two bottom spacers were packaged together. Each top and

bottom pair of spacers was gamma counted on the Hot Cell 4 gamma spectrometer at AL. The Hot Cell 4 spectrometer consists of a high-purity germanium detector that looks through a 0.762 mm (0.03 in) thick aluminum window and a 25.4 mm (1 in) diameter by 203.2 mm (8 in) long lead collimator mounted in the cell concrete wall as shown in Figure 4. The measured activities from the top and bottom spacers were added together to give the total spacer fission product inventory for each capsule.

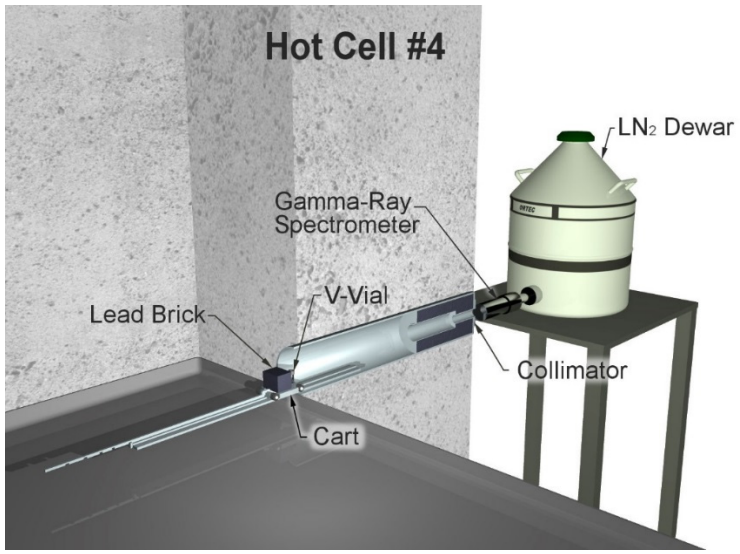

Figure 4. Gamma spectrometry system in Hot Cell 4 at the AL.

2.2 Destructive Analysis Methods

2.2.1 Metallic Hardware: Through Tubes and Capsule Shells

Each capsule had three niobium through tubes that fit in channels in the graphite compact holders to carry capsule instrumentation (i.e., thermocouples and gas lines). The through tubes were attached to the capsule head and bottom. During test train disassembly, the through tubes were destructively separated from the head and bottom, and the head and bottom were separated from the capsule shell (Ploger et al. 2015). The through tubes, capsule heads, capsule bottoms, and capsule shells were transferred to AL for analysis. Negligible activity was detected in the AGR-1 experiment gas lines (Demkowicz et al. 2013); thus, the AGR-2 gas lines were not analyzed. Each component from each capsule was leached separately in near-boiling 8M nitric acid for 30 minutes according to Special Instruction MFC-AL-SI-15-009. After cooling, the components were rinsed with deionized water. The rinse was combined with the leachate. For a given capsule, all the leachates from the different metallic components were combined into a single solution. The solution was counted for gamma-emitting fission products. Solution gamma counting took place at either of two high-purity germanium detectors outside of the hot cell. A separation and gas proportional counting was performed to measure beta-emitting Sr-90. Inductively-coupled plasma-mass spectrometry (ICP-MS) was also performed on the leachate.

2.2.2 Graphite Holders

The Capsule 2, 3, 5, and 6 graphite holders were crushed, transferred from HFEF to AL via pneumatic rabbit, oxidized in air, and the residual ash was acid-leached according to Special Instruction MFC-AL-SI-17-020. For each holder, approximately half of the crushed material was loaded into one plastic “snapcap” container, and the other half was loaded into a second container. Upon receipt at AL, the snapcaps were placed in plastic bags for storage. Prior to analysis, the holder material was removed from the bags and snapcaps for weighing.

The graphite holders were loaded into quartz tall-form beakers and oxidized in the Hot Cell #5 muffle furnace for up to 30 days at about 700°C. A separate beaker was used for each graphite holder. Long oxidation times were required because the borated graphite inhibited oxidation. Inhibited oxidation rates might be from residual B_4C and/or the formation of lithium carbides from neutron transmutation of boron during irradiation. Figure 5 shows the Capsule 3, 6, and 5 graphite holders loaded into tall-form beakers inside the muffle furnace prior to oxidation. Figure 6 shows the residual material after the oxidation step. For all four graphite holders (Capsules 2, 3, 5, and 6), the borated graphite reacted with the quartz beakers, forming bubbles in the quartz, clouding the beakers, and fusing with the beakers. It was hypothesized that borosilicates were formed in the quartz. Part way through the oxidation, the samples were cooled, and the beakers and their contents were placed inside quartz overburden dishes. At some point during the remainder of the oxidation step, the rightmost tall-form beaker in Figure 6 cracked inside of its overburden container. After the oxidation step, a leach was performed according to MFC-AL-SI-17-020. Approximately 100 mL of HNO_3 was added to each overburden dish, and the contents were heated on a hot plate for 30 minutes at near-boiling temperature. The leachate was transferred into a tared 125 mL polyethylene bottle. This process was repeated for a second leach. The leachates were gamma counted, analyzed by inductively-coupled plasma mass-spectrometry (ICP-MS), and separations and counting were performed for Sr-90. Because the ash was fused to the glassware, the post-oxidation weight of the residual ash material could not be measured.

Some additional challenges were faced with the Capsules 2 and 5 graphite holders. Pieces of the crushed Capsule 2 holder had been stored in two plastic snapcap bottles in plastic bags. When the sample was retrieved for analysis, it was found that the snacap containers had crumbled into pieces inside the bags from radiolysis. Sample pieces and the plastic snapcap pieces were transferred into aluminum weighing dishes (see Figure 7). Some powder-like graphite material could not be recovered. Attempts to separate as many plastic pieces from the graphite pieces were made. Thus the initial, pre-oxidation weights are only approximate sample weights. All recovered pieces were oxidized in quartz beakers in the Cell 5 muffle furnace. The borated graphite reacted with the quartz beaker to fuse with the beaker and cause bubbling on the beaker. Attempts to separate the fused material from the beaker using 8M HNO_3 resulted in the beaker breaking before it could be placed in an overburden dish. Some pieces fell on the Cell 5 floor. Recovered pieces were placed in a quartz overburden beaker for two acid leaches according to MFC-AL-SI-17-020.

One of the two plastic containers filled with Capsule 5 graphite holder material also broke. Some of the pieces fell on the Cell 5 floor. The majority of this material was recovered for oxidation and leaching. Because of some losses of Capsule 2 and 5 material, the weights of the holder material at AL prior to oxidation were compared to the calculated pre-irradiation holder weights in Table 3. The right-most column indicates that roughly 14% of the Capsule 2 holder material and 9% of the Capsule 5 holder material may not have been accounted for. The Capsule 3 and 6 weights are also slightly less than 100% of the pre-irradiation calculated masses. It is possible that the measured fission product inventories, particularly in the Capsule 2 holder, could be biased low. Given that PGS scans show asymmetrical distributions of fission products in the holders, it cannot be assumed that the fission product concentrations in the holders are uniform throughout. Therefore, no corrections will be used to account for the missing material.

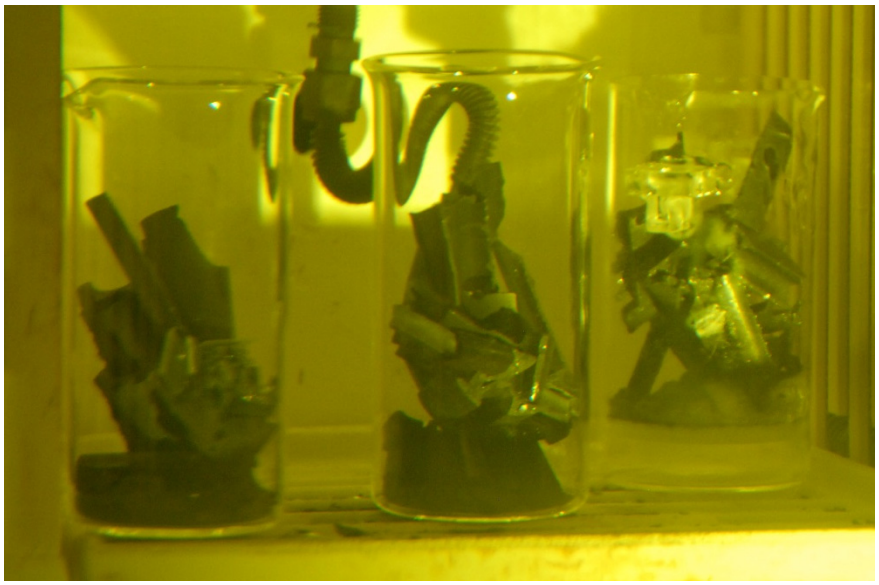

Figure 5. Crushed graphite holders from Capsules 3, 6, and 5 prior to the start of oxidation.

Figure 6. Capsules 3, 6, and 5 graphite holders after oxidation. Tall-form beakers were put inside overburden containers after chemical reactions with the quartz tall-form beakers started.

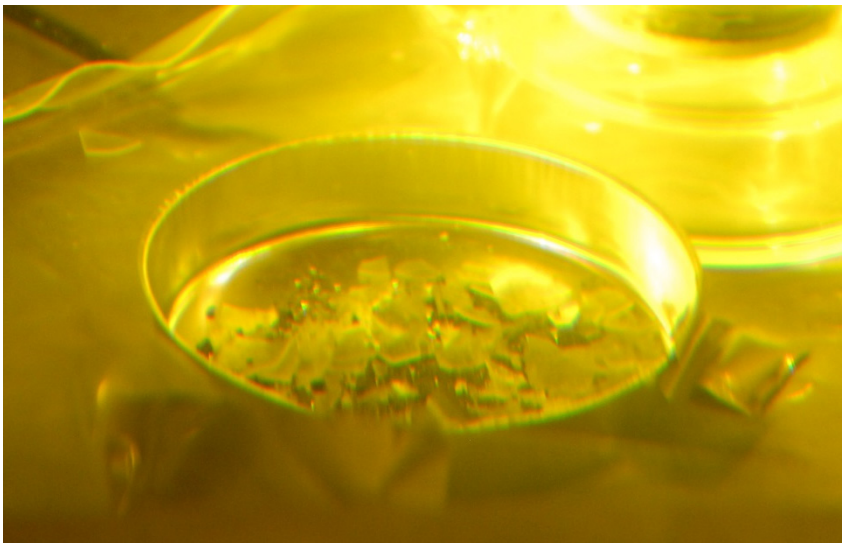

Figure 7. Some of Capsule 2 graphite holder pieces and plastic container in aluminum weighing tray.

Table 3. Comparison of received/recovered graphite holder weights at AL to calculated pre-irradiation weights.

	AL Log #	Container 1 ID	Container 2 ID	Container 1 Weight (g)	Container 2 Weight (g)	Total Graphite Weight (g)	Ratio of Total Graphite Weight to Approx. Pre-irradiation Weight
2	100300	BOTAGR 2-GH02A	BOTAGR 2-GH02B	19.00	20.25	39.25	0.86
3	100303	BOTAGR 2-GH03A	BOTAGR 2-GH03B	21.82	21.41	43.23	0.98
5	100306	BOTAGR 2-GH05A	BOTAGR 2-GH05B	16.18	28.10	44.28	0.91
6	100310	BOTAGR 2-GH06A	BOTAGR 2-GH06B	22.86	20.69	43.55	0.96

2.2.3 Spacers

Europium and strontium are often found to behave similarly in terms of the amount and location of release from the fuel. In Section 3, it will be shown that no Eu-154 was detected on any of the spacers. Therefore the decision was made not to leach the spacers and perform analysis for Sr-90.

3. CAPSULE MASS BALANCE RESULTS

3.1 Calculations with Data and Representation of Results

In Section 3, results for each capsule are presented individually. Comparisons and discussions of the results will follow in Section 0. Detected radioisotope activities were decay-corrected to October 17, 2013 at 11:00 AM MT. This date and time corresponds to the end of the AGR-2 irradiation plus 1 day. Decay corrections were made using the following equation:

$$A = A_o e^{-\lambda t} \quad (1)$$

where A is the activity at time t, A_o is the activity at t= 0, and λ is the decay constant. The decay constant is defined as $\lambda = \ln(2)/t_{1/2}$, where $t_{1/2}$ is the half-life. Half-lives for each isotope were taken from the ENDF/B-VII.1 library downloaded on July 9, 2013 (Chadwick et al. 2011). In instances where no activity was detected for a given isotope, minimum detectable activities (MDAs) were determined. These MDAs were also decay-corrected and should be considered an upper bound on the activity of a given isotope. To calculate the capsule fractions, decay-corrected activities for each isotope were divided by the total activity of that isotope predicted from physics calculations (Sterbentz 2014) to have been produced during irradiation. Capsules 2, 5, and 6 had UCO fuel with 3176 particles per compact and 12 compacts per capsule. Thus, 1 particle is equal to a capsule fraction of 2.62E-5 in these three capsules. Capsule 3 had UO_2 fuel where each of the 12 compacts had 1543 particles. This means that in Capsule 3, 1 particle is equivalent to a capsule fraction of 5.40E-5.

In the following sections (Sections 3.2 through 3.5), one table is given for the capsule hardware (spacers, metallic hardware, and compact holder), and one table is given for the measurement error expressed as a percentage. The metallic hardware includes the through tubes, capsule head and bottom, and capsule shell. The column labeled “Total (measured only)” is the sum of the measured (detected) activities from each component. This column represents a lower bound on the inventory of a given isotope. When a given isotope was not detected, an MDA was determined. The column “Total (measured + MDA)” gives the sum of all measured (detected) values and any values derived from MDAs. This column represents an “upper bound” on the possible inventory of a fission product. In the columns for the spacers, metallic hardware, and compact holders, cells are shaded for cases where a value was derived directly from an MDA. In the two totals columns, a cell is shaded if contribution from MDAs accounts for greater than 50% of the total from the sum of the measured values plus MDAs. With these two totals representing upper and lower bounds, the true total value of the inventory of an isotope lies somewhere between. For example, in Table 6 for Capsule 3, Eu-154 was not detected on any of the capsule components; therefore, the sum of the measured values (lower bound) is zero, but the capsule fraction derived from the sum of the Eu-154 MDAs is 3.79E−4 (upper bound). In this example of Capsule 3, there is considerable uncertainty in the true value of Eu-154 that may exist on the capsule hardware (0 to 3.79E−4).

In addition to the tables summarizing the mass balance of selected isotopes, a table for each capsule is provided that summarizes the measurement error for each isotope on each component. The two right-most columns in the error tables are the propagated relative error of the sums of all the measured values (values for which there was detectable activity). Column “Error of Sum (minus)” is the lower uncertainty bound, and column “Error of Sum (plus)” is the upper uncertainty bound. Note that, in some cases, the uncertainty is asymmetrical (i.e., the upper bound uncertainty is higher than the lower bound uncertainty). This is due to the reported uncertainty from the PGS counts of the compact holders (Harp et al. 2016a, Harp et al. 2016b). Where no activity was detected in any component, a measurement uncertainty cannot be determined, and the cell is labeled “N/D”.

Sections 3.2 through 3.5 report on the inventories of selected isotopes (Ag-110m, Ce-144, Cs-134, Cs-137, Eu-154, and Sr-90) measured outside of the fuel compacts on various capsule components. Section 3.6 summarizes the total fraction of the selected isotopes that were released from the fuel in each

capsule. Greater emphasis is placed on Eu-154 versus Eu-155. Eu-154 has higher-energy gamma rays that are often more readily detectible (and typically with lower error) than Eu-155 in AGR PIE. The measured Cs-137 and Cs-134 are generally in good agreement, but due to trace contamination of the longer-lived Cs-137 in the hot cell, Cs-137 readings are usually biased higher than Cs-134.

3.2 Capsule 2

Table 4 shows the decay-corrected activities, capsule fractions, and particle equivalents for selected isotopes. Table 5 represents the relative measurement errors corresponding to the values given in Table 4. Cells are shaded in Table 4 for cases where a value was derived directly from an MDA.

Table 4. Capsule 2 mass balance for selected isotopes.

Capsule 2	Top Spacer	Bottom Spacer	Metallic Hardware	Compact Holder	Total (measured + MDA)	Total (measured only)
Decay-Corrected Activity (Bq)						
Ag-110m	1.59E+08	7.53E+07	6.03E+08	2.44E+08	1.08E+09	1.08E+09
Cs-134	4.78E+05	2.62E+05	7.33E+06	1.13E+07	1.94E+07	1.94E+07
Cs-137	3.47E+04	1.54E+04	7.76E+06	1.78E+07	2.56E+07	2.56E+07
Ce-144	3.79E+05	5.56E+05	2.82E+06	N/D	3.75E+06	2.82E+06
Eu-154	2.15E+04	8.56E+03	2.90E+05	3.02E+08	3.02E+08	3.02E+08
Sr-90	N/A	N/A	1.28E+07	2.10E+09	2.11E+09	2.11E+09
Capsule Fraction						
Ag-110m	6.91E-02	3.27E-02	2.62E-01	1.06E-01	4.70E-01	4.70E-01
Cs-134	2.16E-06	1.18E-06	3.31E-05	5.10E-05	8.74E-05	8.74E-05
Cs-137	1.72E-07	7.65E-08	3.85E-05	8.82E-05	1.27E-04	1.27E-04
Ce-144	2.06E-07	3.02E-07	1.53E-06	N/D	2.04E-06	1.53E-06
Eu-154	2.63E-06	1.05E-06	3.56E-05	3.70E-02	3.70E-02	3.70E-02
Sr-90	N/A	N/A	7.57E-05	1.24E-02	1.25E-02	1.25E-02
Particle Equivalents						
Ag-110m	2.63E+03	1.25E+03	9.98E+03	4.03E+03	1.79E+04	1.79E+04
Cs-134	8.22E-02	4.52E-02	1.26E+00	1.94E+00	3.33E+00	3.33E+00
Cs-137	6.56E-03	2.92E-03	1.47E+00	3.36E+00	4.84E+00	4.83E+00
Ce-144	7.83E-03	1.15E-02	5.83E-02	N/D	7.77E-02	5.83E-02
Eu-154	1.00E-01	4.00E-02	1.36E+00	1.41E+03	1.41E+03	1.41E+03
Sr-90	N/A	N/A	2.88E+00	4.74E+02	4.76E+02	4.76E+02

N/A: not available because analysis was not carried out.
N/D: not detected

Table 5. Measurement error for each component and propagated measurement error for the sums of detected values.

Capsule 2	Top Spacer	Bottom Spacer	Metallic Hardware	Compact Holder (minus)	Compact Holder (plus)	Error of Sum (minus)	Error of Sum (plus)
Ag-110m	3.0%	3.0%	3.0%	0.4%	0.9%	1.7%	1.8%
Cs-134	3.0%	3.0%	3.0%	2.7%	6.2%	1.9%	3.8%
Cs-137	N/D	N/D	7.0%	1.7%	2.8%	2.4%	2.9%
Ce-144	N/D	N/D	8.0%	N/D	N/D	8.0%	8.0%
Eu-154	N/D	N/D	N/D	0.4%	0.5%	0.4%	0.5%
Sr-90	N/A	N/A	3.0%	1.7%	1.7%	1.7%	1.7%

N/A: not available because analysis was not carried out.
N/D: not detected, error estimate not possible.

3.3 Capsule 3

Table 6 shows the decay-corrected activities, capsule fractions, and particle equivalents for selected isotopes. Table 7 represents the relative measurement errors corresponding to the values given in Table 6. Cells are shaded for cases where a value was derived directly from an MDA or for cases where MDAs account for greater than 50% of the value of a sum of multiple measurements.

Table 6. Capsule 3 mass balance for selected isotopes.

Capsule 3	Top Spacer	Bottom Spacer	Metallic Hardware	Compact Holder	Total (measured + MDA)	Total (measured only)
Decay-Corrected Activity (Bq)						
Ag-110m	2.48E+04	8.92E+03	1.28E+07	2.94E+08	3.06E+08	3.06E+08
Cs-134	1.79E+05	1.34E+05	3.59E+05	2.30E+06	2.97E+06	3.13E+05
Cs-137	2.64E+03	3.19E+03	3.59E+05	3.00E+05	6.65E+05	6.65E+05
Ce-144	1.80E+04	1.80E+04	2.65E+06	N/D	2.68E+06	0
Eu-154	8.54E+02	1.28E+03	2.08E+05	2.10E+06	2.31E+06	0
Sr-90	N/A	N/A	1.26E+07	4.69E+05	1.30E+07	1.30E+07
Capsule Fraction						
Ag-110m	1.06E-05	3.82E-06	5.50E-03	1.26E-01	1.31E-01	1.31E-01
Cs-134	1.12E-06	8.37E-07	2.25E-06	1.44E-05	1.86E-05	1.96E-06
Cs-137	1.98E-08	2.39E-08	2.69E-06	2.25E-06	4.98E-06	4.98E-06
Ce-144	1.59E-08	1.59E-08	2.34E-06	N/D	2.37E-06	0
Eu-154	1.40E-07	2.10E-07	3.41E-05	3.45E-04	3.79E-04	0
Sr-90	N/A	N/A	1.22E-04	4.57E-06	1.27E-04	1.27E-04
Particle Equivalents						
Ag-110m	1.97E-01	7.08E-02	1.02E+02	2.33E+03	2.43E+03	2.43E+03
Cs-134	2.07E-02	1.55E-02	4.16E-02	2.66E-01	3.44E-01	3.62E-02
Cs-137	3.67E-04	4.43E-04	4.98E-02	4.16E-02	9.23E-02	9.23E-02
Ce-144	2.95E-04	2.94E-04	4.32E-02	N/D	4.38E-02	0
Eu-154	2.60E-03	3.89E-03	6.31E-01	6.38E+00	7.02E+00	0
Sr-90	N/A	N/A	2.27E+00	8.46E-02	2.35E+00	2.35E+00

N/A: not available because analysis was not carried out.
N/D: not detected

Table 7. Measurement error for each component and propagated measurement error for the sums of detected values.

Capsule 3	Top Spacer	Bottom Spacer	Metallic Hardware	Compact Holder (minus)	Compact Holder (plus)	Error of Sum (minus)	Error of Sum (plus)
Ag-110m	7.0%	7.0%	3.0%	0.5%	1.2%	0.5%	1.2%
Cs-134	3.0%	3.0%	N/D	N/D	N/D	2.1%	2.1%
Cs-137	7.0%	8.0%	11.0%	33.3%	533.3%	16.2%	240.6%
Ce-144	N/D	N/D	N/D	N/D	N/D	N/D	N/D
Eu-154	N/D	N/D	N/D	N/D	N/D	N/D	N/D
Sr-90	N/A	N/A	3.0%	1.4%	1.4%	2.9%	2.9%
N/A: not available because analysis was not carried out. N/D: not detected, error estimate not possible.							

3.4 Capsule 5

Table 8 shows the decay-corrected activities, capsule fractions, and particle equivalents for selected isotopes. Table 9 represents the relative measurement errors corresponding to the values given in Table 8 Cells are shaded for cases where a value was derived directly from an MDA or for cases where MDAs account for greater than 50% of the value of a sum of multiple measurements.

Table 8. Capsule 5 mass balance for selected isotopes.

Capsule 5	Top Spacer	Bottom Spacer	Metallic Hardware	Compact Holder	Total (measured + MDA)	Total (measured only)
Decay-Corrected Activity (Bq)						
Ag-110m	1.66E+06	2.61E+05	1.43E+07	1.44E+09	1.46E+09	1.46E+09
Cs-134	1.33E+05	1.53E+05	1.80E+06	6.70E+06	8.78E+06	8.78E+06
Cs-137	1.38E+04	1.68E+04	2.44E+06	1.16E+07	1.41E+07	1.41E+07
Ce-144	3.65E+04	1.89E+04	2.61E+06	N/D	2.67E+06	0
Eu-154	1.28E+03	1.72E+03	1.66E+05	2.00E+05	3.69E+05	2.00E+05
Sr-90	N/A	N/A	8.42E+06	1.96E+06	1.04E+07	1.04E+07
Capsule Fraction						
Ag-110m	7.99E-04	1.26E-04	6.90E-03	6.96E-01	7.04E-01	7.04E-01
Cs-134	6.64E-07	7.61E-07	8.97E-06	3.34E-05	4.38E-05	4.38E-05
Cs-137	7.13E-08	8.67E-08	1.26E-05	5.99E-05	7.26E-05	7.26E-05
Ce-144	2.01E-08	1.04E-08	1.44E-06	N/D	1.47E-06	0
Eu-154	1.70E-07	2.28E-07	2.20E-05	2.66E-05	4.90E-05	2.66E-05
Sr-90	N/A	N/A	5.15E-05	1.20E-05	6.35E-05	6.35E-05
Particle Equivalents						
Ag-110m	3.05E+01	4.80E+00	2.63E+02	2.65E+04	2.68E+04	2.68E+04
Cs-134	2.53E-02	2.90E-02	3.42E-01	1.27E+00	1.67E+00	1.67E+00
Cs-137	2.72E-03	3.30E-03	4.79E-01	2.28E+00	2.77E+00	2.77E+00
Ce-144	7.66E-04	3.97E-04	5.48E-02	N/D	5.60E-02	0
Eu-154	6.50E-03	8.69E-03	8.40E-01	1.01E+00	1.87E+00	1.01E+00
Sr-90	N/A	N/A	1.96E+00	4.57E-01	2.42E+00	2.42E+00

N/A: not available because analysis was not carried out.
N/D: not detected

Table 9. Measurement error for each component and propagated measurement error for the sums of detected values.

Capsule 5	Top Spacer	Bottom Spacer	Metallic Hardware	Compact Holder (minus)	Compact Holder (plus)	Error of Sum (minus)	Error of Sum (plus)
Ag-110m	3.0%	3.0%	3.0%	0.1%	0.2%	0.1%	0.2%
Cs-134	3.0%	3.0%	5.0%	4.5%	13.4%	3.6%	10.3%
Cs-137	5.0%	4.0%	7.0%	2.6%	3.4%	2.5%	3.1%
Ce-144	N/D	N/D	N/D	N/D	N/D	N/D	N/D
Eu-154	N/D	N/D	N/D	50.0%	800.0%	50.0%	800.0%
Sr-90	N/A	N/A	3.0%	2.7%	2.7%	2.5%	2.5%
N/A: not available because analysis was not carried out. N/D: not detected, error estimate not possible.							

3.5 Capsule 6

Table 10 shows the decay-corrected activities, capsule fractions, and particle equivalents for selected isotopes. Table 11 represents the relative measurement errors corresponding to the values given in Table 10. Cells are shaded for cases where a value was derived directly from an MDA or for cases where MDAs account for greater than 50% of the value of a sum of multiple measurements.

Table 10. Capsule 6 mass balance for selected isotopes.

Capsule 6	Top Spacer	Bottom Spacer	Metallic Hardware	Compact Holder	Total (measured + MDA)	Total (measured only)
Decay-Corrected Activity (Bq)						
Ag-110m	1.00E+06	1.06E+07	2.03E+08	1.11E+08	3.26E+08	3.26E+08
Cs-134	9.35E+04	1.20E+05	4.19E+05	4.50E+06	5.13E+06	4.71E+06
Cs-137	9.22E+03	3.86E+03	2.45E+05	9.70E+06	9.96E+06	9.95E+06
Ce-144	3.67E+04	5.65E+04	1.99E+06	N/D	2.08E+06	1.99E+06
Eu-154	4.28E+03	2.57E+03	2.49E+05	1.10E+06	1.36E+06	0
Sr-90	N/A	N/A	8.19E+06	7.13E+07	7.95E+07	7.95E+07
Capsule Fraction						
Ag-110m	9.85E-04	1.04E-02	1.99E-01	1.09E-01	3.20E-01	3.20E-01
Cs-134	7.98E-07	1.03E-06	3.58E-06	3.84E-05	4.38E-05	4.02E-05
Cs-137	5.99E-08	2.51E-08	1.59E-06	6.30E-05	6.47E-05	6.47E-05
Ce-144	2.31E-08	3.55E-08	1.25E-06	N/D	1.31E-06	1.25E-06
Eu-154	9.17E-07	5.51E-07	5.34E-05	2.36E-04	2.91E-04	0
Sr-90	N/A	N/A	6.09E-05	2.11E-05	8.21E-05	8.21E-05
Particle Equivalents						
Ag-110m	3.75E+01	3.96E+02	7.60E+03	4.16E+03	1.22E+04	1.22E+04
Cs-134	3.04E-02	3.92E-02	1.36E-01	1.46E+00	1.67E+00	1.53E+00
Cs-137	2.28E-03	9.56E-04	6.06E-02	2.40E+00	2.47E+00	2.46E+00
Ce-144	8.79E-04	1.35E-03	4.76E-02	N/D	4.98E-02	4.76E-02
Eu-154	3.49E-02	2.10E-02	2.04E+00	8.98E+00	1.11E+01	0
Sr-90	N/A	N/A	2.32E+00	8.06E-01	3.13E+00	3.13E+00

N/A: not available because analysis was not carried out.
N/D: not detected

Table 11. Measurement error for each component and propagated measurement error for the sums of detected values.

Capsule 6	Top Spacer	Bottom Spacer	Metallic Hardware	Compact Holder (minus)	Compact Holder (plus)	Error of Sum (minus)	Error of Sum (plus)
Ag-110m	3.0%	3.0%	3.0%	0.7%	2.1%	1.9%	2.0%
Cs-134	3.0%	3.0%	N/A	4.4%	15.6%	4.2%	14.8%
Cs-137	5.0%	N/D	19.0%	2.1%	4.1%	2.1%	4.0%
Ce-144	N/D	N/D	18.0%	N/D	N/D	18.0%	18.0%
Eu-154	N/D	N/D	N/D	N/D	N/D	N/D	N/D
Sr-90	N/A	N/A	3.0%	1.6%	1.6%	1.5%	1.5%
N/A: not available because analysis was not carried out. N/D: not detected, error estimate not possible.							

3.6 Summary of Inventories Released from Fuel

The total fractions of selected fission products released from the fuel compacts in each capsule are summarized below in Table 12. This is a compilation of the fractions that were presented for each individual capsule in the preceding four sections. In Table 12, green shading denotes the rows comprised only of measured results. Orange shading denotes the rows comprised of a sum of the measured results and values derived from MDAs. In those rows, gray shading was used when MDAs account for greater than 50% of the value of the sum for a particular isotope in a particular capsule. Table 13 compiles the measurement relative errors for the values presented in the "Total (measured only)" rows in Table 12.

In some cases in Table 12, there are significant differences between the "Total (measured only)" and "Total (measured + MDA)" values. This is due to the fact that these sums are from multiple different capsule components (e.g., capsule shells, spacers, through tubes, and compact holders) that were analyzed using different methods. For example, the through-tubes for each capsule were leached and the leachate gamma counted at detectors outside of the AL hot cells; the spacers were counted using the stationary sample holder for the Hot Cell 4 spectrometer; the compact holders were counted on the PGS; and Sr-90 was measured from a separation and subsequent proportional counting. Each technique, sample type (geometry), and location has different MDAs and backgrounds that contribute to the uncertainty in the true inventory.

Table 12. Summary of the total fraction of selected isotopes released from the fuel compacts in each capsule.

Capsule Fractions		Ag-110m	Cs-134	Cs-137	Ce-144	Eu-154	Sr-90
Capsule 2	Total (measured + MDA)	4.70E-1	8.74E-5	1.27E-4	2.04E-6	3.70E-2	1.25E-2
	Total (measured only)	4.70E-1	8.74E-5	1.27E-4	1.53E-6	3.70E-2	1.25E-2
Capsule 3	Total (measured + MDA)	1.31E-1	1.86E-5	4.98E-6	2.37E-6	3.79E-4	1.27E-4
	Total (measured only)	1.31E-1	1.96E-6	4.98E-6	0.00E+0	0.00E+0	1.27E-4
Capsule 5	Total (measured + MDA)	7.04E-1	4.38E-5	7.26E-5	1.47E-6	4.90E-5	6.35E-5
	Total (measured only)	7.04E-1	4.38E-5	7.26E-5	0.00E+0	2.66E-5	6.35E-5
Capsule 6	Total (measured + MDA)	3.20E-1	4.38E-5	6.47E-5	1.31E-6	2.91E-4	8.21E-5
	Total (measured only)	3.20E-1	4.02E-5	6.47E-5	1.25E-6	0.00E+0	8.21E-5
N/A: not available because analysis was not carried out. N/D: not detected							

Table 13. Relative error of the total measured fractions given in Table 12.

Relative Error of Fractions in Table 12		Ag-110m	Cs-134	Cs-137	Ce-144	Eu-154	Sr-90
Capsule 2	**Error of Sum (minus)**	1.7%	1.9%	2.4%	8.0%	0.4%	1.7%
	Error of Sum (plus)	1.8%	3.8%	2.9%	8.0%	0.5%	1.7%
Capsule 3	**Error of Sum (minus)**	0.5%	2.1%	16.2%	N/D	N/D	2.9%
	Error of Sum (plus)	1.2%	2.1%	240.6%	N/D	N/D	2.9%
Capsule 5	**Error of Sum (minus)**	0.1%	3.6%	2.5%	N/D	50.0%	2.5%
	Error of Sum (plus)	0.2%	10.3%	3.1%	N/D	800.0%	2.5%
Capsule 6	**Error of Sum (minus)**	1.9%	4.2%	2.1%	18.0%	N/D	1.5%
	Error of Sum (plus)	2.0%	14.8%	4.0%	18.0%	N/D	1.5%
N/D: not detected, error estimate not possible.							

4. DISCUSSION

4.1 Comparison of Compact Holder PGS Results with Burn-leach

While both the PGS (see Section 2.1.2) and burn-leach (see Section 2.2.2) methods measure gamma-emitters in the compact holders, the PGS results are used in preference to the burn-leach gamma results. This is due to the fact that burn-leach recovery of fission products may not be complete. For Sr-90 however, the burn-leach data are used because this beta-emitter cannot be measured in the same manner as gamma emitters. To judge the recovery of isotopes from the burn-leach process, the gamma emitting inventories measured from burn-leach were divided by those measured from PGS in Table 14. For both PGS and burn-leach data, the measured activities were first decay corrected to end of irradiation (EOI)+1 day. In cases where no activity was detected, the MDAs were decay-corrected to EOI+1. The gray shading in Table 14 indicates cases where a value derived from an MDA from the burn-leach data was compared to a measured value from the PGS. The yellow shading indicates a case where the PGS value used in the comparison was derived from an MDA (but the burn leach had measured values), and the brown shading indicates when only an MDA was available from both the PGS and burn-leach.

Ag-110m recovery in Capsules 2, 5, and 6 was 0.18 to 0.19, but in UO_2 Capsule 3, Ag-110m recovery was 0.05. Generally, the ratio of burn-leach Ag-110m to PGS Ag-110m was 2 to 3 times lower in AGR-2 than a similar ratio taken for AGR-1 (Demkowicz et al. 2013).

No Cs-134 was detected from the Capsule 3 holder PGS scans, but a small amount was detected from burn leach. The amount of Cs-137 measured by burn-leach exceeded the PGS measurements of Cs-137 for Capsule 3. This could suggest that the Cs-137 level from burn-leach had been biased high due to hot cell contamination. Capsule 3 contained UO_2 fuel for which very little cesium (on the order of a few percent of one particle inventory) was measured outside of the fuel. The amounts of recovered Cs-134 and Cs-137 were similar within Capsules 2, 5, and 6 (ranging from about 0.4 to about 0.6), and these recoveries were generally similar to AGR-1 (Demkowicz et al. 2013).

AGR PIE has observed that Sr-90 behaves similarly to Eu-154 and Eu-155. The Eu-154 recoveries estimated in Table 14 could be used to infer recovery of Sr-90. The only meaningful measure of Eu-154 recovery from a graphite holder comes from Capsule 2, where the burn-leach measurement of Eu-154 was 26% of that detected from PGS. This Eu-154 ratio for AGR-2 Capsule 2 is between 2 and 6 times lower than those ratios taken in AGR-1. This could be an indication that the Eu-154 and, by extension, the Sr-90 values determined from burn-leach are biased low (at least for Capsule 2). This could be a consequence of the fusing of the compact holder ash with the glassware discussed in Section 2.2.2.

Table 14. Ratio of fraction of selected fission products measured from burn-leach of graphite compact holders to the fraction measured from PGS.

Burn-leach : PGS	Capsule 2	Capsule 3	Capsule 5	Capsule 6
Ag-110m	0.18	0.05	0.19	0.18
Cs-134	0.42	≥ 0.08	0.59	0.64
Cs-137	0.37	5.11	0.37	0.67
Eu-154	0.26	0.04	≤ 0.52	≥ 0.37

Gray: burn-leach MDA compared to measured PGS
Yellow: measured burn-leach compared to PGS MDA
Brown: both burn-leach and PGS values were determined from MDAs

4.2 Silver Mass Balance

Each component of the test train (spacers, metallic hardware, and compact holders) was analyzed for Ag-110m. Figure 8 shows the fraction of Ag-110m measured on each of these three major component groups within the irradiation test train. Totaling the measured Ag-110m across these components gives an estimate of the amount of Ag-110m released from the fuel compacts. The value at the top of each bar in Figure 8 is the sum of all three major components. Fuel compacts are not included in the tallies in Figure 8. In Capsule 2, the Ag-110m was somewhat evenly distributed among the spacers, metallic hardware, and the compact holder. In Capsules 3 and 5, the majority of the Ag-110m outside of the compacts was measured on the compact holders. In Capsule 6, about 20% of the Ag-110m produced in the capsule was measured on the metallic hardware, and an additional 11% was measured in the compact holder.

Each AGR-2 compact was gamma scanned on the PGS (Harp et al. 2016a and Harp et al. 2016b). For each compact, the Ag-110m detected by PGS was compared to the Ag-110m predicted to be produced in that compact from physics calculations (Sterbentz 2014). This gave a measured-to-calculated fraction (M/C) for Ag-110m in each compact. By taking the Ag-110m compacts M/Cs and adding those to the Ag-110m capsule fraction measured on the irradiation test train components (Figure 8), the total Ag-110m mass balance for the AGR-2 irradiation was constructed in Figure 9.

The red values atop each bar in Figure 9 are the total M/Cs for Ag-110m in each capsule. The Ag-110m M/Cs in Capsules 3 and 5 have values > 1.0 indicating that the Ag-110m measured among all the capsule components and the fuel compacts exceeded the amount of Ag-110m predicted to have been produced in these capsules. Ag-110m M/C values > 1.0 were also seen in capsules located toward the axial middle of the AGR-1 and AGR-3/4 irradiation test trains (Demkowicz et al. 2013 and Stempien et al. 2018). This could indicate that the physics calculations may under-predict the production of Ag-110m in capsules near the ATR core axial centerline (such as AGR-2 Capsules 3 and 5).

In Figure 9, the Ag-110m fractions measured for AGR-2 Capsules 2 and 6 are well below 1 at 0.61 and 0.69, respectively. Capsule 2 was near the axial bottom of the test train and Capsule 6 was at the top of the test train. Similarly, lower Ag-110m fractions were measured in the capsules at the extreme top and bottom of the AGR-1 and AGR-3/4 test trains (Demkowicz et al. 2013 and Stempien et al. 2018). The top and bottom capsules from AGR-1 had total Ag-110m M/Cs of 0.76 and 0.89, respectively (lower values than in the other AGR-1 capsules). The top and bottom capsules from AGR-3/4 had total Ag-110m M/Cs of 0.30 and 0.74, respectively (the lowest values in AGR-3/4). In AGR-1 it was determined that the physics calculations tend to over-predict burnup at the top of the test train (Harp 2013), and similar observations were made in AGR-2 (Harp et al. 2016a and Harp et al. 2016b). This would result in an over prediction of the production of Ag-110m in AGR-2 Capsules 2 and 6, and then measured Ag-110m in Capsules 2 and 6 would appear to be under-recovered.

Another factor contributing to the low Ag-110m M/C values for Capsules 2 and 6 in Figure 9 is that the majority of the Ag-110m detected outside of the fuel compacts in those capsules was on the metallic hardware. To measure Ag-110m, the metallic hardware was leached in acid and the leachate was gamma counted (see Section 2.2.1). Sub-optimal recovery of Ag-110m from the leaching process (as was observed for the compact holders in Section 4.1) would result in lower levels of measured Ag-110m on the hardware, and if the majority of the Ag-110m released from the compacts was on the metallic hardware, then the effect of this low recovery on the overall Ag-110m mass balance would be low M/C values, as in the cases of Capsules 2 and 6. In this case, it is not possible to distinguish the extent of over-prediction from the physics calculations from the extent of possible low recovery of Ag-110m from the metallic hardware. Looking at the amount of Ag-110m measured in the compacts themselves may help clarify this.

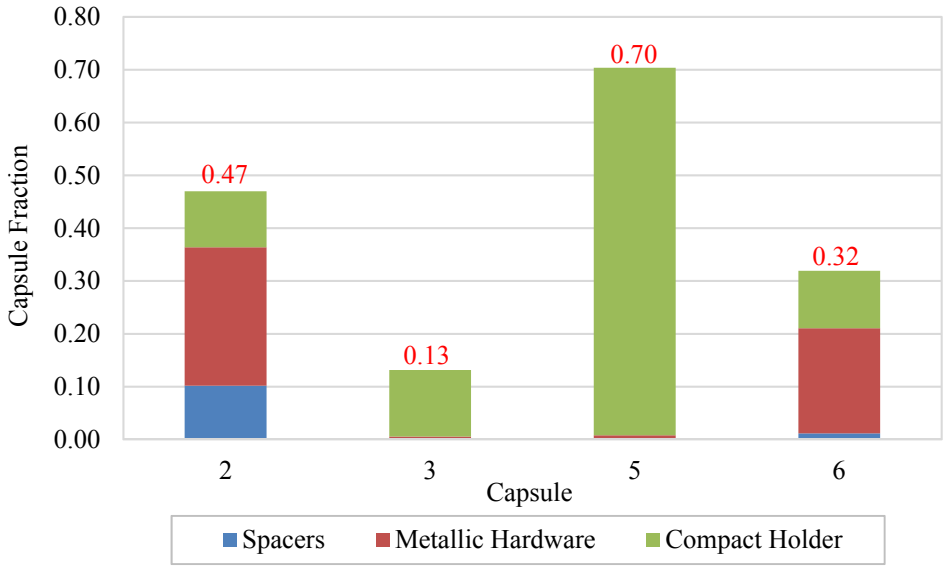

Figure 8. Fractional inventory of Ag-110m measured outside of the fuel compacts.

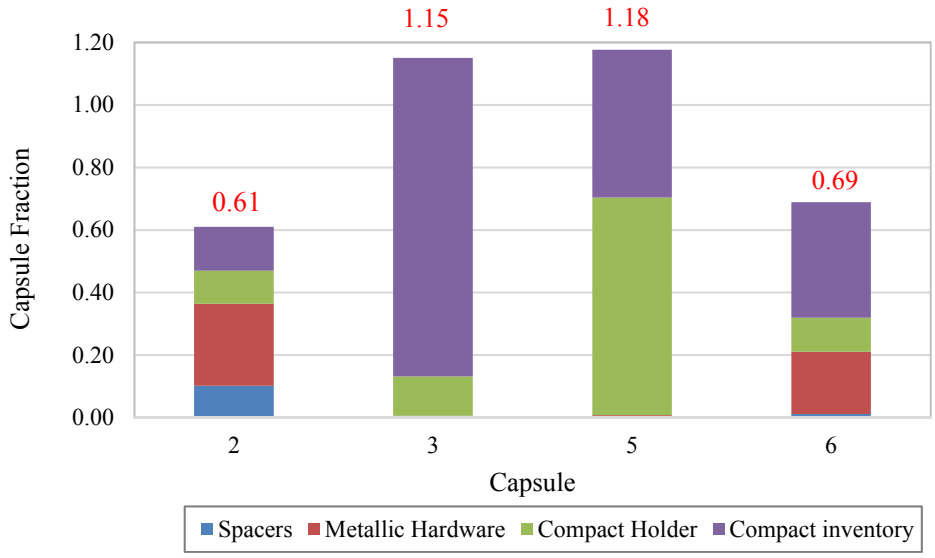

Figure 9. Total inventory of Ag-110m measured across all irradiation capsule components and the fuel compacts compared to Ag-110m production predicted from physics calculations.

Figure 10 shows the total fraction of released Ag-110m as a function of the average compact TAVA irradiation temperature in each capsule. Three representations of the Ag-110m release from compacts are given. The triangles represent the release of Ag-110m from compacts based on summing the Ag-110m activity measured in all compacts within a capsule and dividing by the total activity calculated to have been produced in the capsule. The circles represent the raw fractions calculated from summing the measured Ag-110m fractions outside of the fuel (i.e., on the capsule component spacers, metallic hardware, and compact holders). Ideally, the circles would lie on top of the triangles.

To attempt to account for the bias in the physics prediction, the square symbols in Figure 10 plot the total fractions of Ag-110m measured outside of the fuel on the capsule components and holders after using the total measured Ag-110m values to re-normalize the raw values measured outside of the compact. For any capsule *n*, the equations below describe this normalization process:

$$Compact\ Release_{n,initial} = Holder_n + Spacers_n + Metallic\ Hardware_n$$

$$Compacts = \sum All\ Compacts\ in\ Capsule_n$$

$$Total_{Ag-110m\ measured} = Compact\ Release_{n,initial} + Compacts$$

$$Compact\ Release_{n,renormalized} = \frac{Compact\ Release_{n,initial}}{Total_{Ag-110m\ measured}}$$

Holder$_n$, *Spacers*$_n$, and *Metallic Hardware*$_n$ are the fraction of Ag-110m produced in capsule *n* during irradiation that was measured on those components. *Compacts* is the sum of the Ag-110m decay-corrected activities for each compact divided by the total capsule predicted Ag-110m. This renormalization implicitly assumes that 100% of the silver produced in a given capsule has been measured between the compacts, holders, spacers, and capsule metallic hardware. The success of the re-normalization is based largely on the accuracy of that assumption. With this renormalization, values where $Total_{Ag\text{-}110m\ measured} > 1$ effectively adjust the raw fractions in Figure 10 to lower values for Capsules 3 and 5. Conversely, $Total_{Ag\text{-}110m\ measured}$ for Capsules 2 and 6 was significantly < 1, and this renormalization adjusts the raw fractions upwards in Figure 10. In all cases, the renormalized values lie closer to the compact M/C values.

Combining the observations made from Figure 9 with the results of the renormalization in Figure 10, some conclusions may be drawn. The fact that the renormalized Capsule 2 components values now lie much nearer to the compact M/C value indicates that the Capsule 2 physics calculations may indeed over-predict Ag-110m production. The renormalized Capsule 5 values are now within about 7% of the compact value M/C, indicating that the calculated values may indeed be over-predicting Ag-110m production. The renormalized Capsule 6 value now lies about halfway between the raw value and the compact value. This might indicate that both some calculational over-prediction and under recovery from metallic components had occurred. For Capsule 3, the compact M/C value is > 1 so that 1 - M/C is < 0. This is a clear indication that the physics calculations under-predict Ag-110m production in Capsule 3.

While the triangles in Figure 10 showed 1 minus the capsule-wide compact M/C (this is the fraction of Ag-110m released from the compacts assuming the predicted inventory is accurate), Figure 11 shows the M/C values (representing the amount of Ag-110m retained in the fuel compacts if the predicted inventory is correct) for each AGR-2 compact versus the compact TAVA irradiation temperature. With Ag-110m M/Cs significantly < 1 for many compacts (especially in UCO Capsules 2, 5, and 6), it is clear that release through intact TRISO coatings was the dominant release mechanism for silver. It is notable that the amount of Ag-110m measured outside of the fuel compacts plateaus beginning at around 1100°C in Figure 10. Accordingly, the amount of Ag-110m remaining in the compacts (Figure 11) reaches its lowest values for compact TAVA temperatures equal to or greater than 1100°C. This could be related to a rapid increase in the silver diffusion rate through intact SiC layers at intermediate temperatures ranging from approximately 1100 to 1300°C observed during post-irradiation heating testing (Hunn et al. 2015).

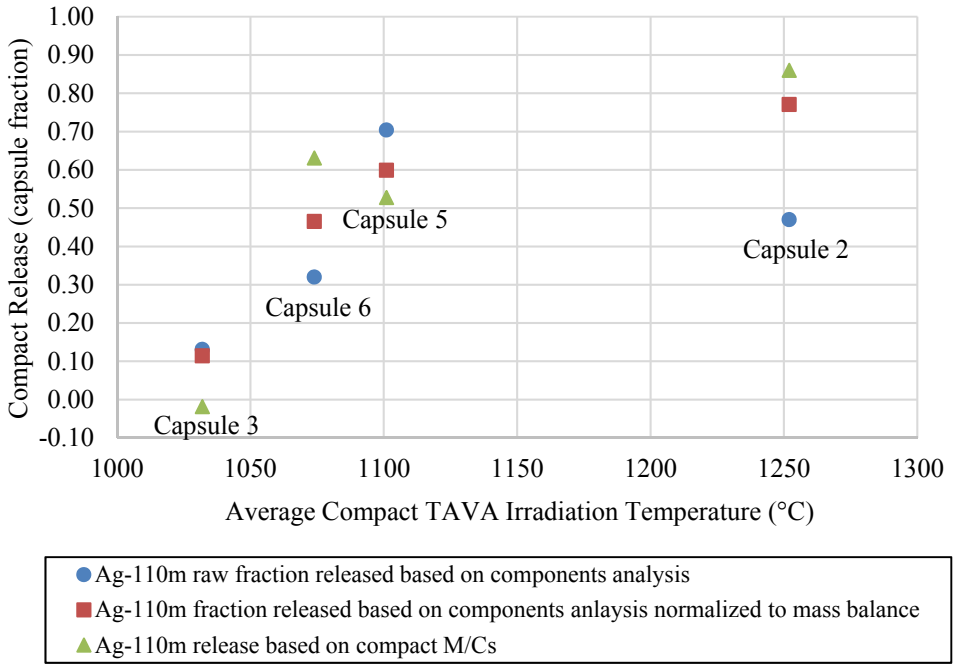

Figure 10. Three representations of the fraction of Ag-110m measured outside of the fuel compacts as a function of the compact-averaged TAVA irradiation temperature.

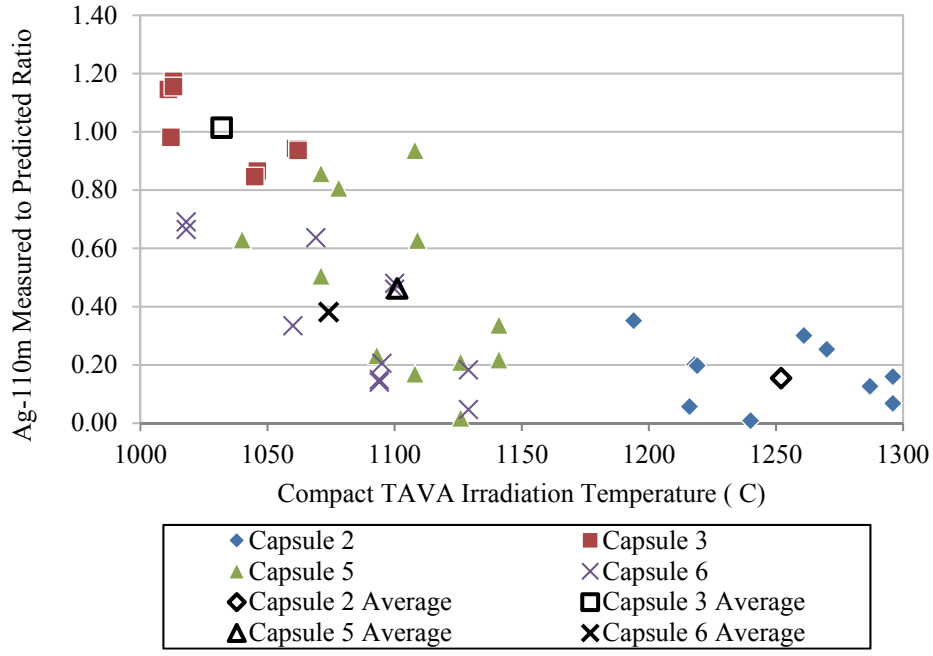

Figure 11. Measured-to-calculated Ag-110m fraction in each compact in each capsule versus compact TAVA irradiation temperature.

4.3 Cesium Mass Balance

Capsule components were analyzed for both Cs-134 and Cs-137. As mentioned earlier, results for Cs-134 are chosen to represent cesium because Cs-137 is more susceptible to bias from hot cell contamination. Figure 12 shows the breakdown of Cs-134 inventories on capsule components outside of the fuel compacts. Patterned fill indicates that a value is either derived from an MDA or is a sum of measured values and MDAs where the MDAs account for greater than 50% of the sum. In Capsule 2, Cs-134 was detected on all components. Destructive PIE confirmed that nickel metal contamination of the SiC layers in at least four Compact 2-2-3 particles (likely due to a failed thermocouple sheath in that capsule) resulted in SiC layer degradation that contributed to cesium releases (Hunn et al. 2018). In Capsule 3, Cs-134 was detected on the spacers, but MDAs were used for the metallic hardware and compact holders where no Cs-134 was detected. Referring back to Table 6 for Capsule 3, the high-estimate for total Cs-134 measured outside of the compacts is a capsule fraction of 1.86E-5. This is the value depicted in Figure 12. The "low-estimate", based entirely on measured values only, with no MDAs, is 1.96E-6. An important point is that patterned fill indicates that MDAs are the majority of the value, but that does not mean that no Cs-134 was detected. To see the low-estimate values comprised solely of measured values, refer back to the summary in Table 12 or the tables specific to each capsule in Section 3. No MDAs comprise the Capsule 5 results, but an MDA was used for the metallic hardware in Capsule 6. For each capsule, the majority of the Cs-134 released from the fuel was measured on the compact holders, and significant amounts were measured on the metallic hardware in Capsules 2 and 5.

It has been observed in AGR-1 PIE that cesium is not released in significant fractions unless there is degradation of the SiC layer of one or more particles (Hunn et al. 2016). A particle with a failed SiC layer will release a significant amount of its cesium inventory (generally 20 to 100%) (Hunn et al. 2016). Consequently, measured cesium is often expressed in units of particle inventories. Table 15 summarizes the number of particles worth of cesium measured outside of the fuel compacts in each capsule. A compact with a failed SiC particle will not necessarily release all of the cesium from that particle (Hunn et al. 2016). Some could be retained in the fuel kernel, and some could be retained in the compact matrix but outside of the particle. Greater than one particle's worth of Cs-134 was measured outside of the fuel compacts for Capsules 2, 5, and 6. That is a good indication that there were some failed-SiC particles or particles with as-fabricated, defective SiC coatings in those capsules.

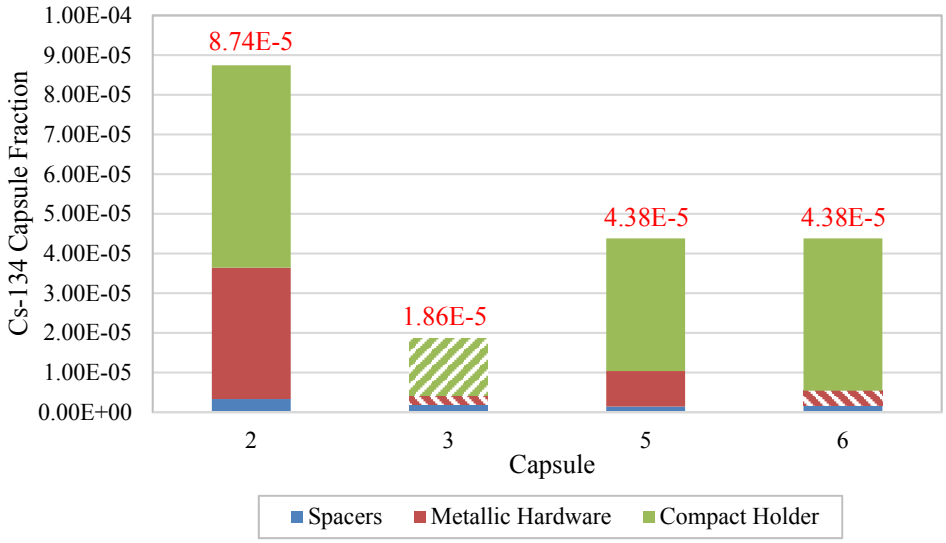

Figure 12. Fractional inventory of Cs-134 measured outside of the fuel compacts. Patterned fill indicates values derived from MDAs.

Table 15. Summary of the number of particles' worth of Cs-134 outside of the fuel compacts in each capsule. These values were excerpted from Table 4, Table 6, Table 8, and Table 10.

Capsule	Total Particle Equivalents (measured + MDA)	Total Particle Equivalents (measured only)
2[a]	3.33	3.33
3[b]	0.344	0.0362
5[a]	1.67	1.67
6[a]	1.67	1.53
a. One particle in Capsules 2, 5, and 6 is equivalent to a capsule fraction of 2.62E-5. b. One particle in Capsule 3 is equivalent to a capsule fraction of 5.40E-5.		

4.4 Europium and Strontium Mass Balances

All capsule components (i.e. spacers, metallic hardware, and compact holders) were analyzed for gamma-emitting Eu-154 and Eu-155. As stated earlier, Eu-154 was used in preference to Eu-155 to represent europium because Eu-154 has higher-energy gamma rays that are more readily detectible (and typically with lower error) than Eu-155 in AGR PIE. Only the metallic hardware and compact holders were analyzed for Sr-90. Because no Eu-154 was detected on the spacers, the spacers were not leached and analyzed for Sr-90 (see Section 2.2.3).

There are a couple sources of bias and/or error in the measurements. In the holders, Eu-154 was determined from gamma scanning on PGS and should have relatively low systematic error. In comparison, Sr-90 was measured in the holders by the destructive burn-leach process described in Section 2.2.2. This method requires the ash of the holder remaining after oxidation be dissolved in a nitric acid solution, where Sr-90 recovery may not be 100%. Thus, systematic uncertainty (which is unknown) in the Sr-90 values in the compact holders may be larger than for Eu-154. It is possible that the Sr-90 values in the compact holders may be biased low in all capsules. In the metallic hardware, both Eu-154 and Sr-90 were analyzed by leaching the metallic hardware in acid (see Section 2.2.1). No Eu-154 was detected from any of the metallic hardware leaches. If the recovery if Eu-154 and/or Sr-90 from these components was incomplete, then both the Eu-154 and Sr-90 values could be biased low on the metallic hardware as well.

Figure 13 shows the distribution of Eu-154 across all of the components outside of the fuel compacts. The figure at left is scaled to better show the magnitude of the Eu-154 fractions in Capsule 2, and the figure at right better shows the Eu-154 fractions for Capsules 3, 5, and 6. Eu-154 was detected exclusively in the Capsule 2 and 5 compact holders. The error on the Capsule 2 Eu-154 measurement was about 0.5% (see Table 5), but the error on the Eu-154 measurement in the Capsule 5 holder was -50%/+800%.[b] No Eu-154 was measured outside of the compacts for Capsules 3 and 6; however, MDAs were used to determine an upper bound on Eu-154 compact releases in these capsules.

Figure 14 shows the distribution of Sr-90 measured on the metallic hardware and compact holders. Sr-90 is measured using different methods than the gamma counting used for Eu-154. Leaching, chemical separation, and gas proportional counting for Sr-90 offer a higher sensitivity than gamma counting for Eu-154 in these samples; thus, Sr-90 was detected on all metallic hardware and all holders from all capsules. In addition to Eu-154, significant release of Sr-90 through intact TRISO coatings was also observed in Capsule 2.

[b] The PGS method often results in asymmetrical error (Harp et al. 2016b).

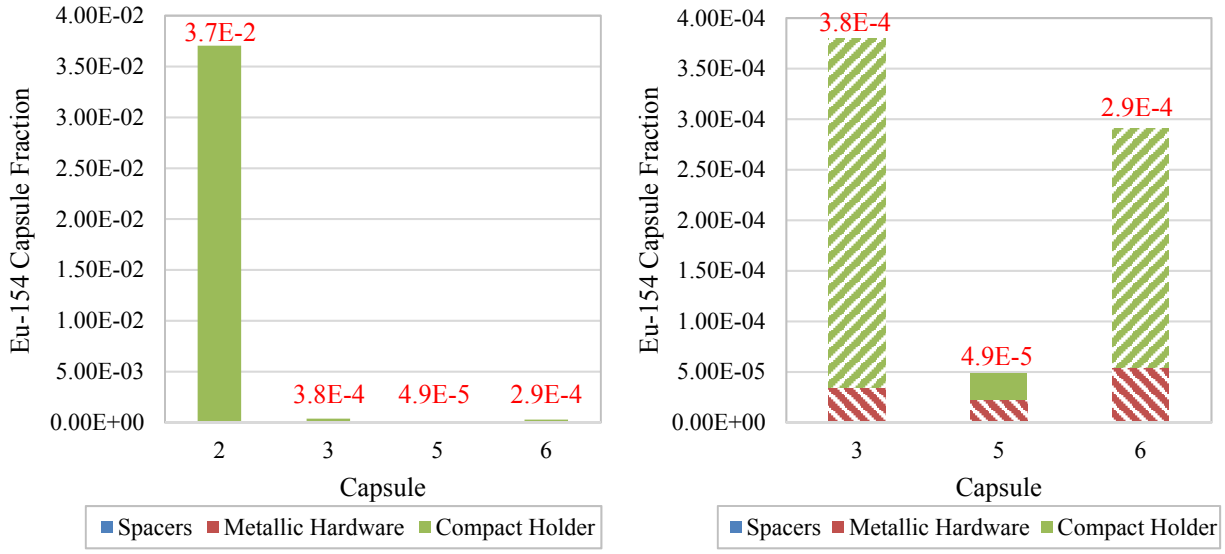

Figure 13. Capsule fractions of Eu-154 measured on components outside of the fuel compacts. Left: highlights Capsule 2. Right: highlights Capsules 3, 5, and 6. Patterned fill indicates values derived from MDAs.

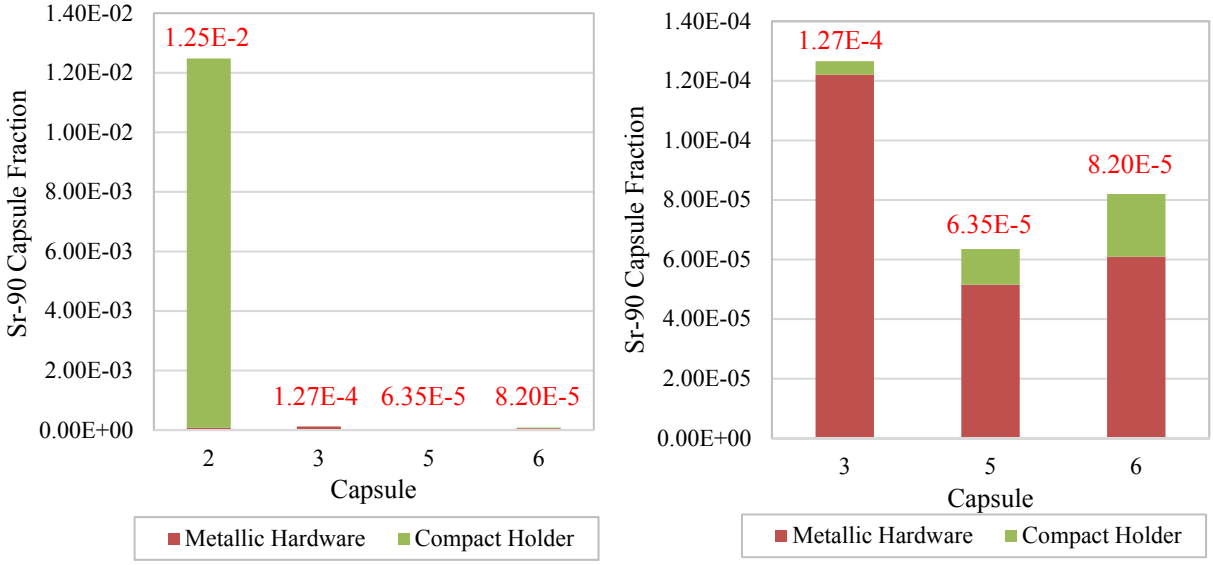

Figure 14. Capsule fractions of Sr-90 measured on components outside of the fuel compacts. Left: highlights Capsule 2. Right: highlights Capsules 3, 5, and 6.

Within Capsules 2 and 5, the amounts of Sr-90 measured outside of the compacts were within about a factor of three of the Eu-154. From Table 8, the capsule fractions of Eu-154 and Sr-90 measured outside of the compacts in Capsule 5 are 2.66E-5 (1.01 particle equivalents) and 6.35E-5 (2.42 particle equivalents), respectively. From Table 4, the amounts of Eu-154 and Sr-90 released from Capsule 2 compacts are 3.7E-2 and 1.25E-2, respectively. In Capsule 2, those fractions are equivalent to about 1410 particles' worth of Eu-154 and 476 particles worth of Sr-90. This indicates significant release of both Eu-154 and Sr-90 through intact TRISO coatings in Capsule 2, which was the hottest capsule in the AGR-2 experiment, with a TAVA temperature of 1252°C (150 to 220°C hotter than the other capsules).

Comparing the Sr-90 measured outside of the compacts for UO_2 Capsule 3 and UCO Capsules 5 and 6 shows that UO_2 and UCO retain Sr-90 similarly for TAVA compact irradiation temperatures from 1032 to 1100°C in AGR-2. In Capsules 5, 6, and 3, the Sr-90 fractional releases were 6.35E-5, 8.21E-5, and 1.27E-4, respectively. The Eu-154 releases (including contributions from MDAs) were <2.9E-4, 4.9E-5, and <3.8E-4, for Capsules 6, 5, and 3, respectively. This precludes a meaningful comparison between UO_2 and UCO Eu-154 retention.

Figure 15 shows the fraction of Eu-154 and Sr-90 measured outside of the fuel compacts as a function of the average compact TAVA irradiation temperature in each capsule. Open symbols indicate values dominated by MDAs. The Eu-154 and Sr-90 values tend to follow each other. As mentioned in the preceding paragraphs, the recovered Sr-90 from burn-leach of the holders could have biased the measured Sr-90 to lower values. For Capsules 3, 5, and 6, with compact TAVA temperatures between 1000 and 1100°C, the releases from fuel were similar at fractions of roughly 1E-4. AGR-1 Capsules 1 and 4 had TRISO coatings similar to AGR-2, compact TAVA temperatures between 1050 and 1070°C, and Eu-154 release fractions of 1.3E-4 and 1.4E-4, respectively (Demkowicz et al. 2015). But for AGR-2 Capsule 2 at 1252°C, the Eu-154 and Sr-90 releases jumped to 3.7% and 1.25%, respectively. A similar temperature dependence for Eu-154 releases was observed in AGR-3/4 (Stempien et al. 2018), where Eu-154 releases were similar for temperature between 800 and 1200°C, but increased significantly for compact TAVA temperatures greater than 1200°C. AGR-3/4 Capsule 7 (compact-averaged TAVA temperature 1345°C) had a Eu-154 release of 3.2%, compared to 3.7% release for AGR-2 Capsule 2 (compact-averaged TAVA temperature 1252°C). While AGR-3/4 Capsule 7 was hotter than AGR-2 Capsule 2, the AGR-2 irradiation was longer (559 effective-full-power-days) than the AGR-3/4 irradiation (369 effective-full-power-days). This could explain the similar quantities of Eu-154 release observed in these two capsules from two different irradiations.

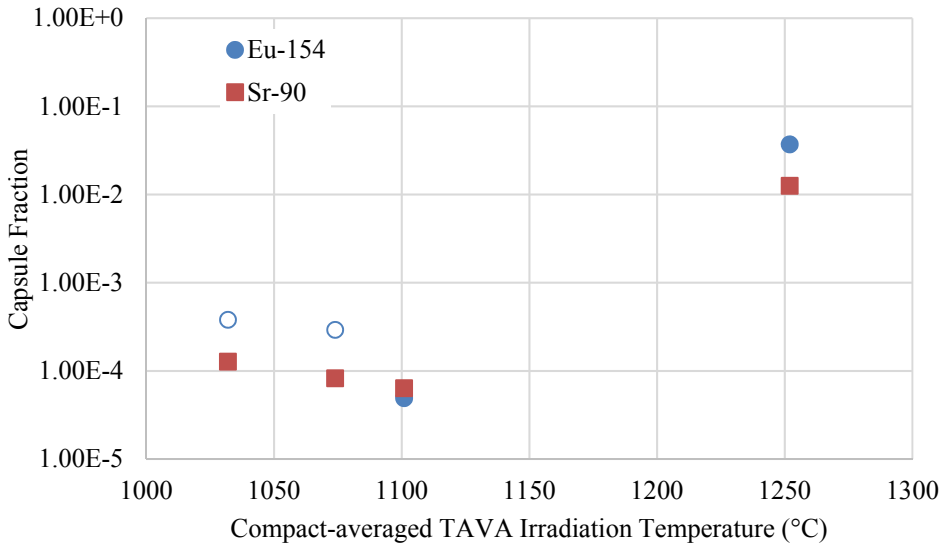

Figure 15. Fractions of Eu-154 and Sr-90 measured outside of the fuel compacts as a function of the compact-averaged TAVA irradiation temperature. Open symbols for Eu-154 indicate values derived from MDAs.

5. CONCLUSIONS AND FUTURE WORK

Major conclusions from the AGR-2 fission product mass balance are as follows:

- Components of the irradiation test train (e.g., capsule hardware, holders, spacers etc.) were analyzed for gamma-emitting fission products, especially isotopes of Ag, Cs, Ce, and Eu. Components were also analyzed for beta-emitting Sr-90.
- Ag-110m was significantly released through intact TRISO coatings in all capsules. It was measured on every component in each of the U.S. AGR capsules (Capsules 2, 3, 5, and 6). Releases from the fuel compacts ranged from 13% for Capsule 3 to 70% for Capsule 5.
- Ag-110m releases increase sharply going from compact TAVA irradiation temperatures of about 1025°C (11% release) to 1100°C (60% release). The Ag-110m release at 1250°C was about 75%.
- Given the temperature dependence of silver transport and the fact that there was only one capsule with UO_2 fuel, it cannot be determined from the data whether UCO or UO_2 fuel retain silver differently.
- Measured Cs-134 releases from the fuel compacts ranged from a fraction of about 4.0E-5 to 8.7E-5 (1.5 to 3.3 particle equivalents) in the UCO fuel. Destructive PIE confirmed that nickel metal contamination of the SiC layers in some Compact 2-2-3 particles (likely due to a failed thermocouple sheath in that capsule) resulted in some SiC layer failures that contributed to cesium releases. A fraction of 1.96E-6 (0.036 particle equivalents) was measured outside of the generally lower-burnup/lower-temperature UO_2 fuel compacts in Capsule 3.
- In the UCO fuel, no Eu-154 was detected outside of the compacts in Capsule 6; however, using the estimated MDA as an upper bound suggests that releases were < 2.91E-4. A Eu-154 fraction of 2.66E-5 was detected outside of the compacts in Capsule 5 (the upper bound estimate was < 4.9E-5). In Capsule 2, there was 3.7% Eu-154 release. This is evidence of release through intact TRISO coatings at the Capsule 2 compact TAVA irradiation temperature of 1252°C (150 to 220°C hotter than the other capsules).
- In capsules where both Eu-154 and Sr-90 were detected outside of fuel compacts, their fractions were within a factor of 3.
- No Eu-154 was detected outside of the UO_2 fuel compacts in Capsule 3; thus, applying an MDA gives Capsule 3 releases of < 3.79E-4.
- Sr-90 fractions of 8.21E-5, 6.35E-5, and 1.25E-2 were measured outside of the fuel compacts in Capsules 6, 5, and 2, respectively. In UO_2 Capsule 3, a fraction of 1.27E-4 was released from the compacts. These data suggest that UCO and UO_2 retain Sr-90 similarly for irradiation temperatures of 1100°C or less.
- Plotting Sr-90 releases versus compact TAVA irradiation temperature shows that compact releases for temperatures from about 1025 to 1100°C were very similar, at around 1E-4; however, the release at 1250°C was 3.7E-2. This suggests that there is an acceleration of Sr-90 release at irradiation temperatures greater than about 1200°C.

This report has focused on fission product inventories outside of AGR-2 fuel compacts. Comparing these results to predicted fission product production in the compacts gives an estimate of the fraction of fission products released from the fuel compacts. Also of interest is the quantity of fission products that were released from the fuel particles, but retained within the compact matrix. Compacts have been selected for as-irradiated destructive analysis to determine the inventory retained in the matrix. Combining this with the measured inventories outside of the fuel compacts can give an estimate of the total fission product inventory released from the fuel particles. Some fuel compacts with potential SiC or TRISO failures were selected for as-irradiated, destructive analyses to attempt to identify and quantify particles with defective coatings.

6. REFERENCES

Chadwick, M. B., et al., 2011, "ENDF/B-VII.1 Nuclear Data for Science and Technology: Cross-Sections, Covariances, Fission Product Yields and Decay Data," *Nuclear Data Sheets*, Vol. 112, pp. 2887–2996 specific decay data accessed 2013-07-09 at http://www.nndc.bnl.gov/endf/b7.1/.

Collin, B.P., 2015a, *AGR-1 Irradiation Test Final As-Run Report*, INL/EXT-10-18097, Rev. 3, Idaho National Laboratory, January 2015.

Collin, B.P., 2015b, *AGR-3/4 Irradiation Test Final As-Run Report*, INL/EXT-15-35550, Rev. 0, Idaho National Laboratory, June 2015.

Collin, B.P., 2018a, *AGR-2 Irradiation Test Final As-Run Report*, INL/EXT-14-32277, Rev. 4, Idaho National Laboratory, February 2018.

Collin, B.P., 2018b, "AGR-5/6/7 Irradiation Experiment Test Plan," PLN-5245, Rev. 1, Idaho National Laboratory, January 2018.

Demkowicz, P. A., Harp, J. M., Winston, P. L., and S.A. Ploger, 2013, *Analysis of Fission Products on the AGR-1 Capsule Components*, INL/EXT-13-28483, Idaho National Laboratory, March 2013.

Demkowicz, P. A., 2013, "AGR-2 Post-Irradiation Examination Plan," PLN-4616, Rev. 0, Idaho National Laboratory, December 2013.

Demkowicz, P. A., Hunn, J. D., Morris, R. N., van Rooyen, I., Gerczak, T., Harp, J. M. and S.A. Ploger, 2015, *AGR-1 Post-Irradiation Examination Final Report*, INL/EXT-15-36407, Idaho National Laboratory.

Demkowicz, P. A., 2017, "AGR-3/4 Phase 2 Post-Irradiation Examination Plan," PLN-5382, Idaho National Laboratory, May 2017.

Harp, J. M., 2013, "Analysis of Individual Compact Fission Product Inventory and Burnup for the AGR-1 TRISO Experiment Using Gamma Spectrometry," ECAR-1682, Idaho National Laboratory, February 2013.

Harp, J.M., Demkowicz, P.A., and J.D. Stempien, 2016a, *Fission Product Inventory and Burnup Evaluation by Gamma Spectrometry of the AGR-2 Irradiation*, INL/EXT-16-39777, Idaho National Laboratory.

Harp, J.M., Demkowicz, P.A., and J.D. Stempien, 2016b, "Fission Product Inventory and Burnup Evaluation of the AGR-2 Irradiation by Gamma Spectrometry", *Proceedings of the 8th International Topical Meeting on High Temperature Reactor Technology,* Paper 18593, HTR 2016 Las Vegas, NV USA, Nov 6-10, 2016.

Hawkes, G., 2014a, "AGR-1 Daily As-Run Thermal Analyses," ECAR-9638, Rev. 4, September 2014, Idaho National Laboratory.

Hawkes, G., 2014b, "AGR-2 Daily As-Run Thermal Analyses," ECAR-2476, Rev. 1, August 2014, Idaho National Laboratory.

Hunn, J.D. and R.A. Lowden, 2007, *Data Compilation for AGR-3/4 Driver Fuel Coated Particle Composite LEU03-09T*, ORNL/TM-2007/019, Oak Ridge National Laboratory.

Hunn, J.D., Savage, T.W., and Chinthaka Silva, 2010, *AGR-2 Fuel Compact Pre-Irradiation Characterization Summary Report*, ORNL/TM-2010/226, November 2010, Oak Ridge National Laboratory.

Hunn, J.D., Lowden, R.A., Miller, J.H., Jolly, B.C., Trammell, M.P., Kercher, A.K., Montgomery, F.C., and C.M. Silva, 2014, "Fabrication and Characterization of Driver Fuel Particles, Designed-to-Fail Fuel Particles, and Fuel Compacts for the US AGR-3/4 Irradiation Test, *Nuclear Engineering and Design*, Vol. 271, pp. 123-130.

Hunn, J.D., Morris, R.N., Baldwin, C.A., Montgomery, F.C., and T.J. Gerczak, 2015, *PIE on Safety-Tested AGR-1 Compact 4-2-2*, ORNL/TM-2015/033, Oak Ridge National Laboratory.

Hunn, J.D., Baldwin, C.A., Gerczak, T.J., Montgomery, F.C., Morris, R.N., Chinthaka, M.S., Demkowicz, P.A., Harp, J.M., Ploger, S.A., van Rooyen, I., and K.E. Wright, (2016), "Detection and analysis of particles with failed SiC in AGR-1 fuel compacts," *Nuclear Engineering and Design*, Vol. 306, pp. 36-46.

Hunn, J.D., Morris, R.N., Montgomery, F.C., Gerczak, T.J., Skitt, D.J., Baldwin, C.A., Dyer, J.A., Helmreich, G.W., Eckhart, B.D., Burns, Z.M., Demkowicz, P.A., and J.D. Stempien, 2018, "Post-irradiation examination and safety testing of US AGR-2 Irradiation Test Compacts," *Proceedings of the 9th International Topical Meeting on High Temperature Reactor Technology*, HTR 2018, Paper HTR 2018-0010, Warsaw, Poland, October 8-10, 2018.

INL, 2017, "Technical Program Plan for INL Advanced Reactor Technologies Technology Develop Office/Advanced Gas Reactor Fuel Development and Qualification Program," PLN-3636, Revision 6, June 2017, Idaho National Laboratory.

Ploger, S., Demkowicz, P. A., and J.A. Harp, 2015, *AGR-2 Irradiated Test Train Preliminary Inspection and Disassembly First Look*, INL/EXT-15-34997, Idaho National Laboratory, May 2015.

Stempien, J. D., Demkowicz, P. A., Harp, J. M., and P.L. Winston, 2018, *AGR-3/4 Experiment Preliminary Mass Balance*, INL/EXT-18-46049, Idaho National Laboratory, August 2018.

Sterbentz, J.W., 2013, "JMOCUP As-Run Daily Depletion Calculation for the AGR-1 Experiment in ATR B-10 Position," ECAR-958, Rev. 2, September 2013, Idaho National Laboratory.

Sterbentz, J.W., 2014, "JMOCUP As-Run Daily Depletion Calculation for the AGR-2 Experiment in ATR B-12 Position," ECAR-2066, Rev. 2, April 2014, Idaho National Laboratory.

Appendix A

Analytical Laboratory Report Numbers

Appendix A

Analytical Laboratory Report Numbers

Capsule Number	Through Tubes and Capsule Shells (Leach solution gamma, ICP-MS, ICP-OES, and Sr-90)	Top and Bottom Spacers (gamma counting)	Graphite Compact Holder (burn-leach, solution gamma, ICP-MS, and Sr-90)
1	98526	98757	N/A
2	98390	98757	100300
3	98440	98757	100303
4	98535	98757	N/A
5	98407	98757	100306
6	98444	98757	100310